Supporting Information

Biosynthesis of Fluorinated Peptaibols Using a Site Directed Building Block Incorporation Approach

José Rivera-Chávez,[†] Huzefa A. Raja,[†] Tyler N. Graf,[†] Joanna E. Burdette,[‡] Cedric J. Pearce,[§] and Nicholas H. Oberlies[†,*]

†Department of Chemistry and Biochemistry, University of North Carolina at Greensboro, P.O. Box. 26170, Greensboro, North Carolina 27412, United States

‡Department of Medicinal Chemistry and Pharmacognosy, University of Illinois at Chicago, Illinois 60612, United States

§Mycosynthetix, Inc., 505 Meadowlands Drive, Suite 103, Hillsborough, North Carolina 27278, United States

TABLE OF CONTENTS

List of tables

List of schemes

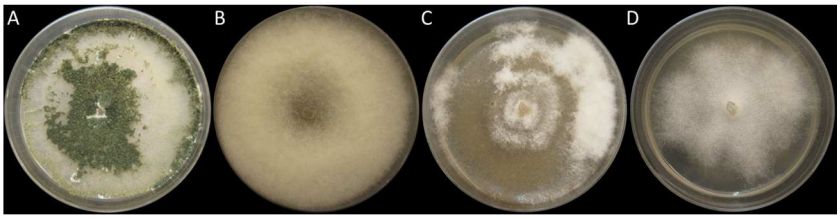

Figure S1. Cultures of MSX70741 (*Trichoderma arundinaceum*) grown on Potato Dextrose Agar (PDA) under four different conditions for 21 days. A) Normal PDA. B) PDA supplemented with *ortho*-F-DL-Phe. C) PDA supplemented with *meta*-F-DL-Phe. D) PDA supplemented with *para*-F-DL-Phe.

Fungal strain isolation and identification

Mycosynthetix fungal strain MSX70741 was isolated from wood collected in a humid mountain forest (April 1993), while strain MSX57715 was isolated from leaf litter in a predominately oak forest (October 1991) both by Dr. Barry Katz.[1] Both strains were used previously for the isolation of peptaibols.[1] At that time, we utilized the D2 region of the 28S rDNA and classified the above two strains only to ordinal level as Hypocreales spp. (GenBank accessions: JN377382 and JN377381, respectively). Based on morphological examination of the strains grown on potato dextrose agar (PDA, Difco), we were able to identify the strains as belonging to the genus *Trichoderma.* In this study, we sequenced three gene regions, specifically the partial fragment of translation elongation factor 1-alpha (*tef1),* the partial region of the second largest subunits of RNA polymerase (*RPB2*), and the ITS1, 5.8S, ITS2 rDNA for the identification of fungal strains, as these loci have been used successfully for the identification of *Trichoderma* spp previously[2,3] and reference strains are available in the RefSeq Database maintained by GenBank[4] for identification via DNA barcoding and DNA-taxonomy approaches. The ITS region was obtained with primers ITS5 and ITS4;[5] the *tef1* region, specifically intron 4 in combination with intron 5, which is useful for species-level identification, was obtained using primer combinations 728F/983F and 986R/2218R;[6,7] while *RPB2* was obtained using primers RPB25f and RPB27cr.[8] Thermocycler parameters and primer sequences for the three regions are outlined in Table S1. Sanger sequencing of the purified PCR products was performed using BigDye Terminator v3.1 cycle sequencing at Eurofins Genomics (https://www.eurofinsgenomics.com). The sequences were obtained bidirectionally using both strands with the same primers used for PCR. Sequences were generated on an Applied Biosystems 3730XL high-throughput capillary sequencer. Sequences were assembled with Sequencher 5.2.3 (Gene Codes), optimized, and then corrected manually when necessary.

The ITS region was sequenced because it has been designated as a barcoding marker for fungi[9] and a reference strain database, International Subcommission on *Hypocrea* and *Trichoderma* (ISHT) TrichoKey and TrichoBLAST has been developed, which helps in identification of *Trichoderma* strains.[10] When we

BLAST searched the ITS sequence of MSX70741 against the ISHT database, the strain was identified as *Trichoderma brevicompactum*, while GenBank BLAST against the RefSeq database revealed 99% similarity with numerous reference strains belonging to species within the "*T. brevicompactum* clade", such as *Trichoderma turrialbense* (GenBank NR_138448; strain CBS 112445), *Trichoderma arundinaceum* (GenBank NR_134372; strain: ATCC 90237), *Trichoderma protrudens* (GenBank NR_134373; strain: CBS 121320), and *Trichoderma rodmanii* (GenBank NR_134374; strain BPI GJS 91-88)). Recent studies have argued that ITS may not provide sufficient resolution for species-level identification within *Trichoderma* and other genera within the order Hypocreales.[11,12] Therefore, we used portions of *tef1* and *RPB2* to obtain a species-level identification of *Trichoderma* spp.[11]

Table S1. PCR protocols and primers used for identification of *Trichoderma* spp.

Locus	Primer	Primer Sequence 5'-3'	Direction	PCR protocol	Reference
Translation elongation factor 1-alpha (*tef1*)	EF1-983F/EF1-728F EF1-986R/EF1-2218R	GCY CCY GGH CAY CGT GAY TTY AT CAT CGA GAA GTT CGA GAA GG TAC TTG AAG GAA CCC TTA CC ATG ACA CCR ACR GCR ACR GTY TG	Forward Forward Reverse	1. 94 °C – 2 min 2. 66 °C – 56 °C touchdown (9 cycles) 3. 94 °C – 30 sec 4. 56 °C – 1 min 5. 72 °C – 1 min 6. Repeat 3-5 for 36 cycles 7. 72 °C – 10 min 8. 4 °C finish	6,7,13
DNA-directed RNA polymerase II subunit 2 (*RPB2*)	RPB2-5f RPB2-7cR	GAY GAY MGW GAT CAY TTY GG CCC ATR GCT TGY TTR CCC AT	Forward Reverse	1. 94 °C – 3 min 2. 94 °C – 20 sec 3. 55 °C – 30 sec 4. 72 °C – 1 min 5. Repeat 2-4 for 40 cycles 6. 72 °C - 10 min 7. 4 °C finish	13
Internal Transcribed Spacer (ITS)	ITS5 ITS4	GGA AGT AAA AGT CGT AAC AAG G TCC TCC GCT TAT TGA TAT GC	Forward Reverse	1. 95 °C – 5 min 2. 94 °C – 30 s 3. 52 °C – 30 s 4. 72 °C – 1 min 5. Repeat 2-4 for 35 cycles 6. 72 °C – 8 min 7. 4 °C finish	14,15

Both the *tef1* and *RPB2* sequences were BLAST searched in GenBank separately, and the top most similar sequences were downloaded and aligned with the sequences of MSX70741 using MUSCLE[16] within the program SeaView v. 4.1. We then employed separate phylogenetic analyses for *tef1* and *RPB2* sequences using Maximum Likelihood with RAxML[16] on the CIPRES server[17] with 1000 bootstrap

replicates to assess branch/clade support for the resulting topology of the phylogenetic tree. Maximum Likelihood analyses using both gene regions (*tef1 and RPB2*) independently placed strain MSX70741 within the *Trichoderma brevicompactum* clade with strong bootstrap support (100% RAxML bootstrap support for *tef1* and 98% RAxML bootstrap support for *RPB2*, respectively). Within the *T. brevicompactum* clade, MSX70741 showed strong phylogenetic affinities to *Trichoderma arundinaceum* (83% RAxML bootstrap support for *tef1* and 100% RAxML bootstrap support for *RPB2*, respectively) (Figure S1). All names used in the phylogenetic analysis conform to recent nomenclature of *Trichoderma* spp[11]. Therefore, based on the results of BLAST search (DNA Barcoding) and Maximum Likelihood analyses (DNA-taxonomy), MSX70741 was identified as *Trichoderma arundinaceum*[2] (Ascomycota; Pezizomycotina; Sordariomycetes; Hypocreomycetidae; Hypocreales; Hypocreaceae). The sequence data for MSX70741 were deposited in GenBank (accession no: ITS: KY630171, *tef1*: KY630169, KY630170, RPB2: KY630166).

For identification of MSX57715, we sequenced *tef1* and *RPB2*, but not the ITS region, as it shows incomplete resolution for species-level identification in *Trichoderma* spp. Based on a BLAST search using GenBank, the closest hits using *tef1* sequences were *Trichoderma albolutescens* (GenBank FJ860609; strain: CBS 119286; Identities = 724/730 (99%), Gaps = 3/730 (0%), and *Trichoderma albolutescens* (GenBank FJ860609; strain: S396; Identities = 720/726 (99%), Gaps = 3/26 (0%)). Further, based on a Maximum Likelihood analysis using *RPB2* sequences by employing RAxML, MSX57715 was identified as *Trichoderma albolutescens* (MSX57715 occurred on a strongly supported clade; 100% RAxML bootstrap support with reference strain GenBank: FJ860517, strain: Ex-type culture: CBS 119286 of *Trichoderma albolutescens*) (Supporting information). The sequence data for MSX57715 were deposited in GenBank (accession no: *tef1*: KY630167, KY630168, RPB2: KY630164, KY630165).

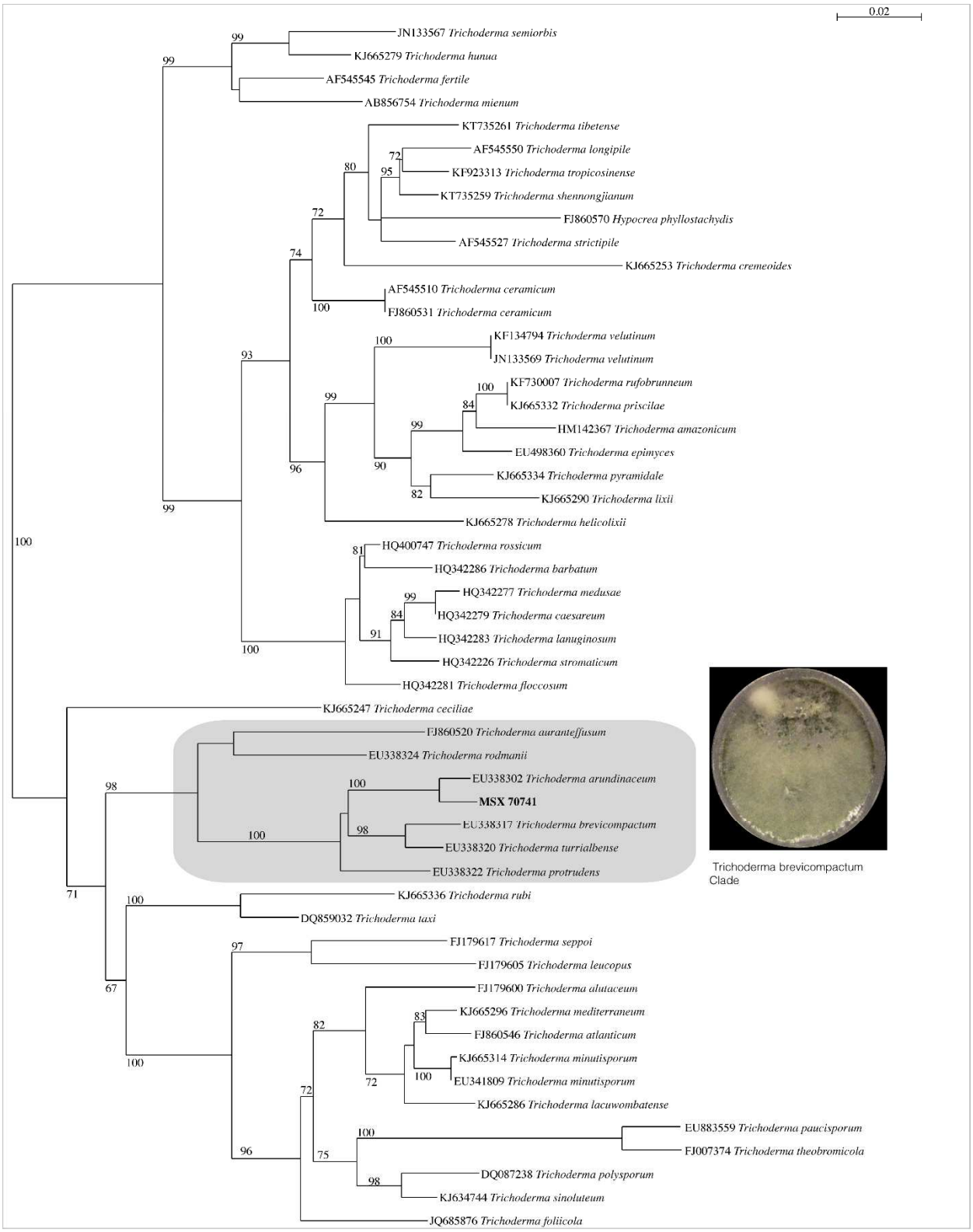

Figure S2. Phylogram of the most likely tree (-lnL = 7876.71) from a RAxML analysis of 52 taxa based on *RPB2* sequence data (1063 bp). Numbers refer to RAxML bootstrap support values ≥ 70% based on 1000 replicates. Strain MSX70741 was identified as *Trichoderma arundinaceum* (Bold, highlighted in gray). A 14 d old culture on Potato Dextrose Agar media is shown. Bar indicates nucleotide substitutions per site.

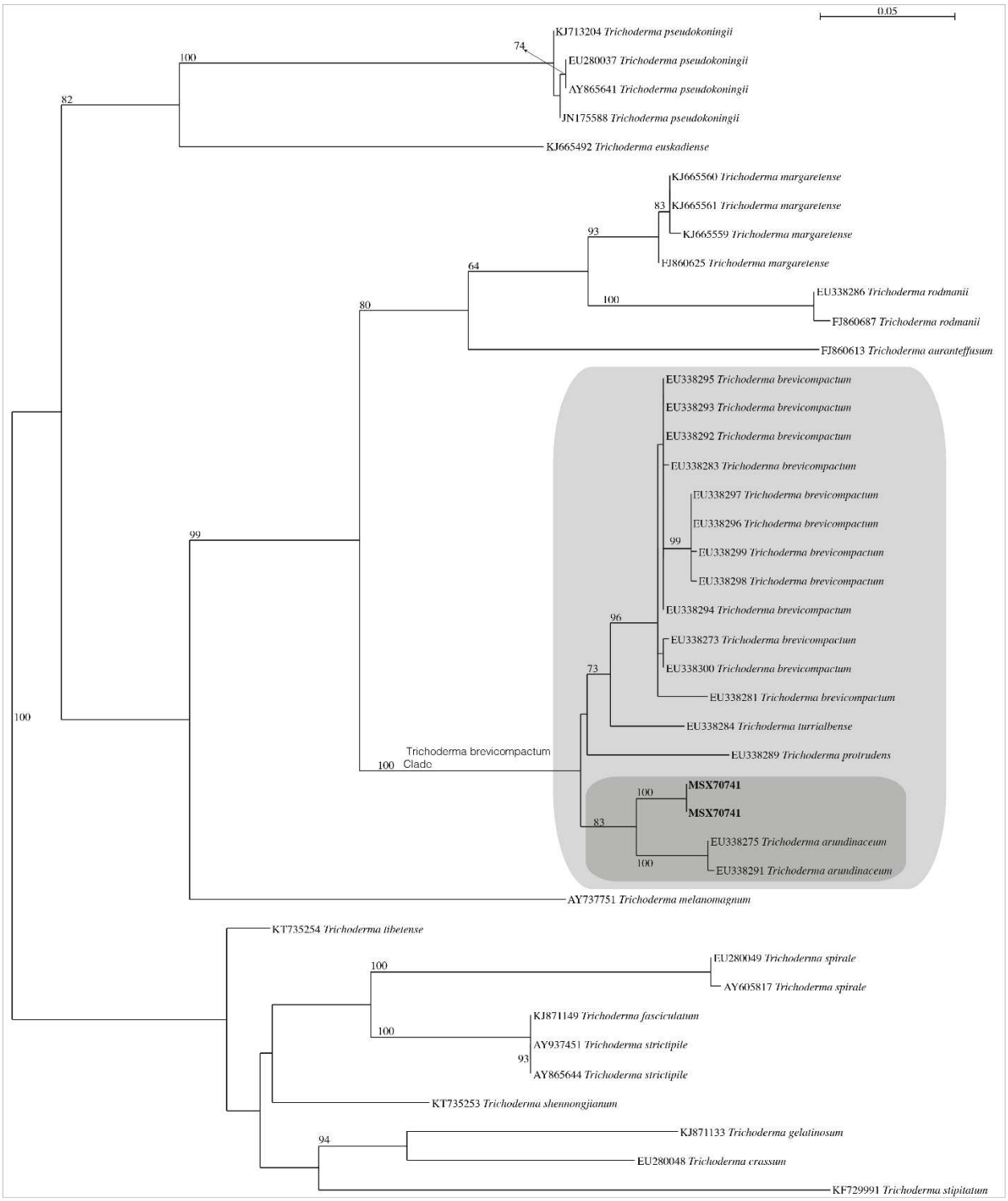

Figure S3. Phylogram of the most likely tree (-lnL = 3836.71) from a RAxML analysis of 41 taxa based on *tef-1* sequence data (518 bp). Numbers refer to RAxML bootstrap support values ≥ 70% based on 1000 replicates. Strain MSX70741 was identified as *Trichoderma arundinaceum* (Bold, highlighted in gray). Bar indicates nucleotide substitutions per site.

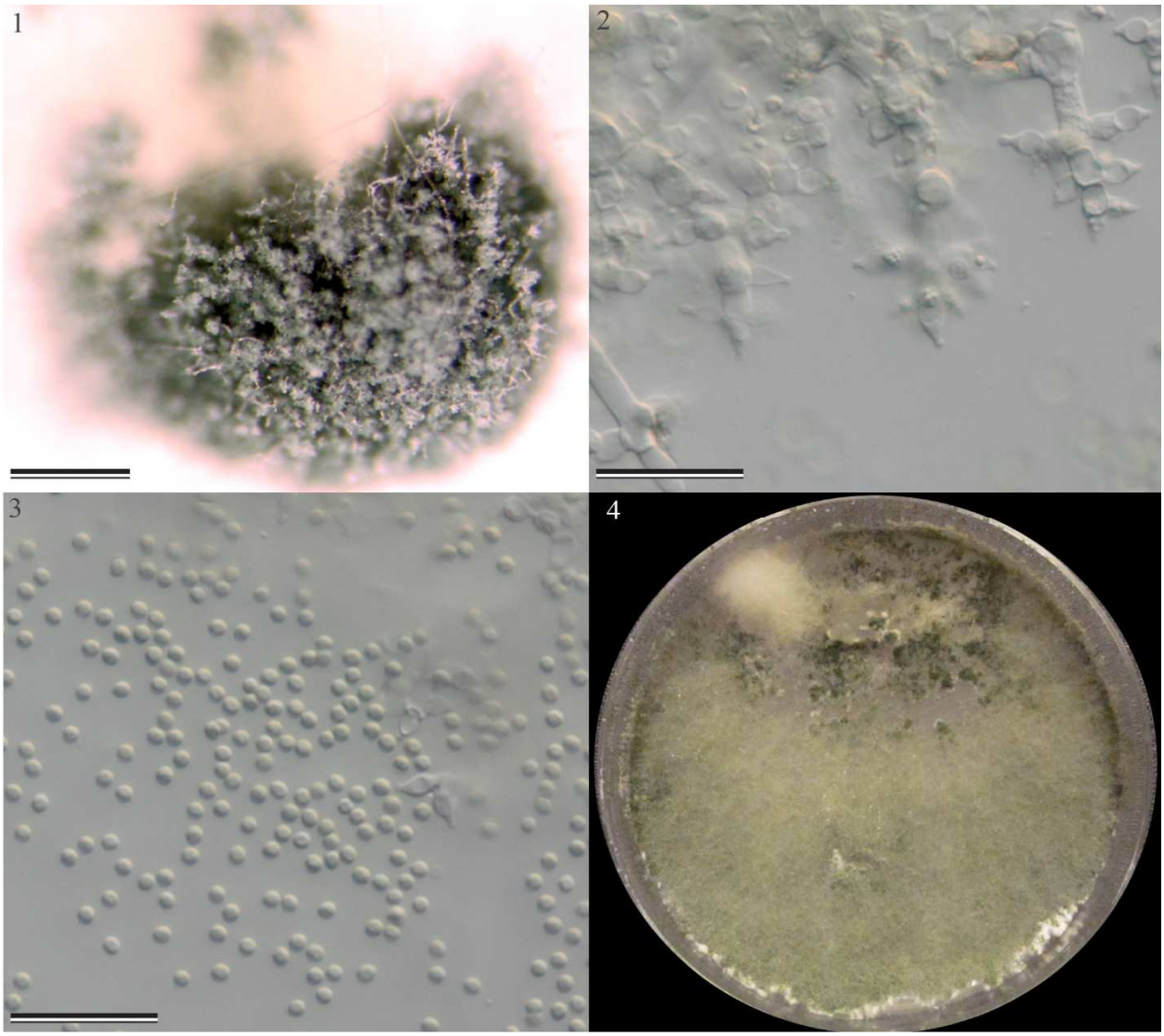

Figure S4. *Trichoderma arundinaceum* (MSX70741). 1. Pustules showing protruding conidiophores. 2. Conidiophore on PDA (Difco). 3. Conidia. 4. 14 d old culture on PDA media; Scale Bars: 1 = 100 µm, 2, 3 = 20 µm.

Figure S5. Phylogram of the most likely tree (-lnL = 9524.67) from a RAxML analysis of 103 taxa based on *RPB2* sequence data (1060 bp). Numbers refer to RAxML bootstrap support values ≥ 70% based on 1000 replicates. Strain MSX57715 was identified as *Trichoderma albolutescens* (highlighted in gray). A 14 d old culture on Potato Dextrose Agar media is shown. Bar indicates nucleotide substitutions per site. *Protocrea farinosa* is used as an outgroup.

Fermentation, extraction and isolation

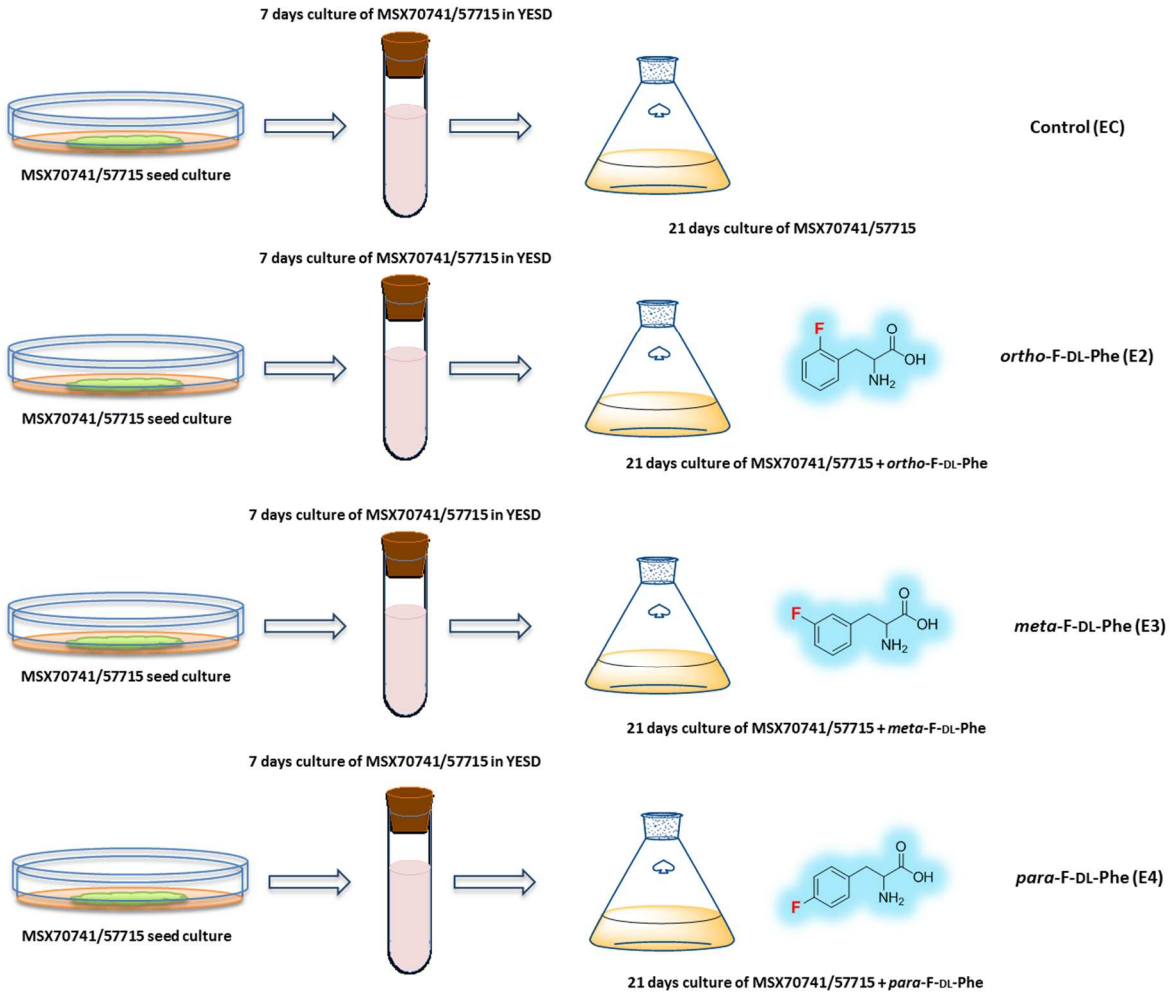

Scheme S1. Culture conditions of MSX70741 and MSX57715 on rice (EC, control) and rice supplemented with a racemic mixture of *ortho*, *meta* or *para*-F-phenylalanine (E2-E4).

Culture conditions optimization

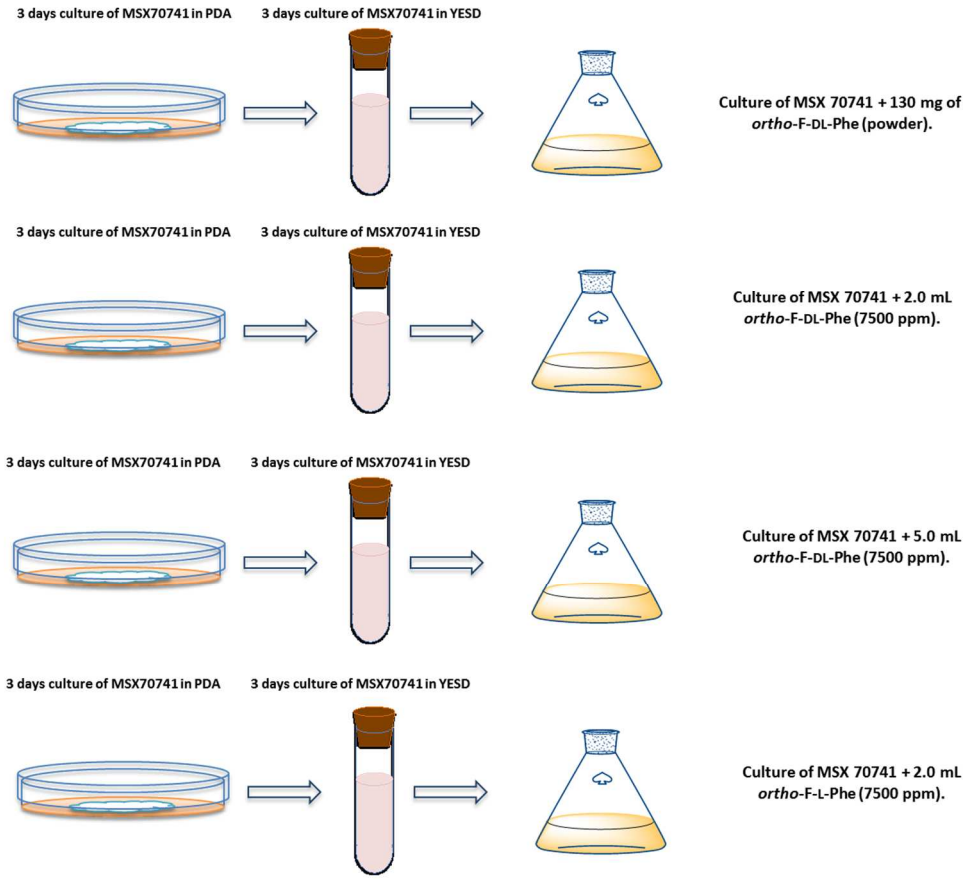

Scheme S2. Experiments designed for optimization of culture conditions for biosynthesis of fluorinated alamethicin F50 analogues.

Preparation of *ortho*-F-Pheol and *meta*-F-Pheol standards

To a suspension of 25 mg of *ortho*-F-D-Phe, *ortho*-F-L-Phe, *meta*-F-D-Phe or *meta*-F-L-Phe (Acros Organics) in 2.5 mL of anhydrous tetrahydrofuran (THF) were added 2.5 mL of a suspension of 15.0 mg of lithium borohydride in 2.5 mL of anhydrous THF. After the addition, the reaction was heated at 65 °C for two hours (Scheme 3) and then cooled to room temperature. Then, the excess of reagent was decomposed by dropwise addition of 2 N aqueous sodium hydroxide and water (5 mL of each). The resulting white solids were collected by filtration and washed with 30 mL of THF (2 ×). The eluent was evaporated *in vacuo*, and the resulting materials were recrystallized from ethyl acetate-hexane 1:1 to give **7**-**10**.

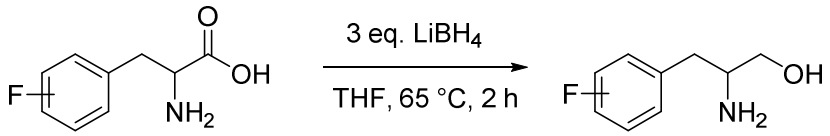

Scheme S3. Synthetic strategy for the preparation of *ortho*-F-Pheol and *meta*-F-Pheol standards.

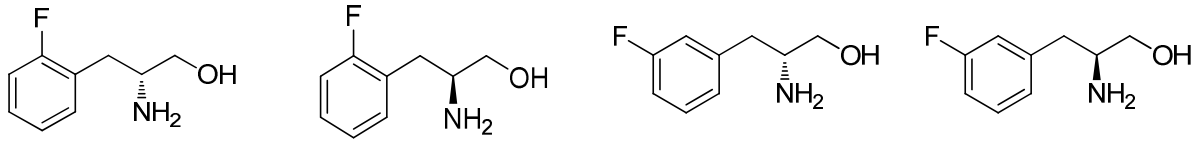

7 **8** **9** **10**

Figure S6. Structures of *ortho*-F-D-pheol (**7**), *ortho*-F-L-pheol (**8**), *meta*-F-D-pheol (**9**), and *meta*-F-L-pheol (**10**).

Table S2. NMR data for *ortho/meta*-F-Phenylalaninol (**8** and **9**). Data recorded in CD_3OH. ^{1}H (500 MHz), ^{13}C (125 MHz) and ^{19}F (470 MHz)

	Compound (**8**)			Compound (**9**)		
Position	δ_C	type	δ_H, m, J (Hz)	δ_C	type	δ_H, m, J (Hz)
1	64.7, *s*	CH_2	a. 3.42, *dd*, (11.0,7.0)	61.2, *s*	CH_2	a. 3.55, *dd*, (11.5, 6.0)
			b. 3.71, *dd*, (11.0, 4.0)			b. 3.71, *dd*, (11.5, 3.5)
2	54.5, *s*	CH	3.22, *m*	55.6, *s*	CH	3.49, *m*
3	32.5, *d*, (1.4)	CH_2	a. 2.78, *dd*, (13.5, 7.0)	35.9, *d*, (1.6)	CH_2	a. 2.99, *dd*, (14.0, 8.5)
			b. 2.89, *dd*, (13.5, 7.0)			b. 3.71, *dd*, (11.5, 6.5)
4	125.8, *d*, (15.8)	C		140.1, *d*, (7.4)	C	
5	162.7, *d* (242.3)	CF		117.2, *d*, (21.5)	CH	7.11, *dt*, (10.0, 2.0)
6	116.4, *d*, (22.1)	CH	7.09, *t*, (9.0)	164.4, *d*, (244.4)	CF	
7	130.0, *d*, (8.1)	CH	7.28, *m*	115.0, *d*, (21.0)	CH	7.01, *td*, (8.5, 2.0,)
8	125.5, *d*, (3.5)	CH	7.14, *t*, (7.5)	131.7, *d*, (8.4)	CH	7.37, *td*, (8.0, 6.5)
9	132.9, *d*, (4.6)	CH	7.28, *t*, (7.5)	126.4, *d*, (2.9)	CH	7.15, *d*, (8.5)
5-F			-119.65, *m*			-
6-F			-			-114.78, *td*, (10.0, 6.5)

Marfey's analysis

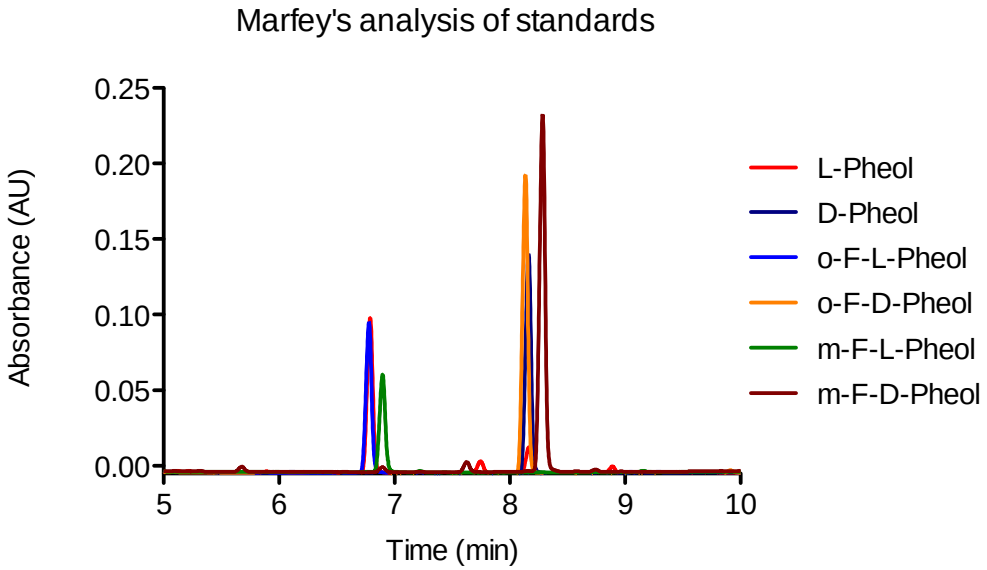

Figure S7. Marfey's analysis of standards.

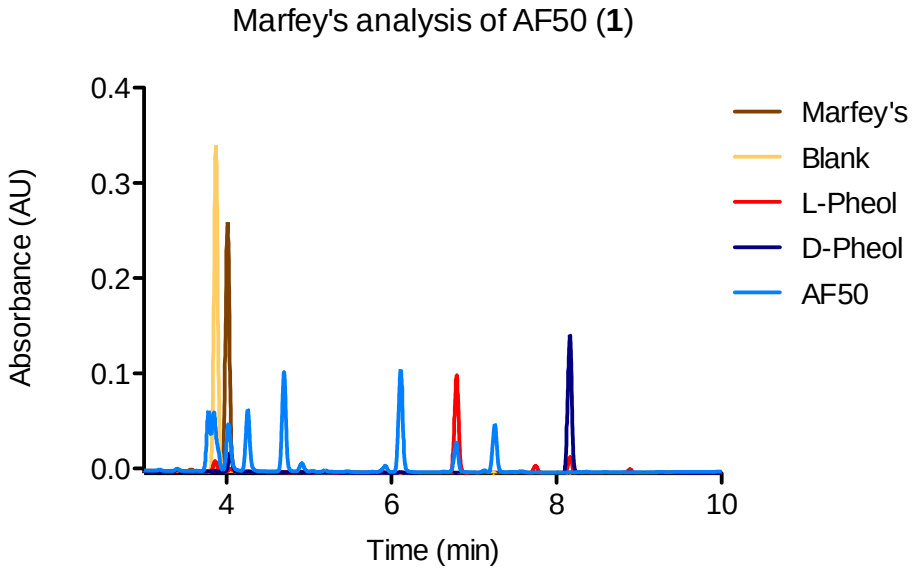

Figure S8. Marfey's analysis of alamethicin F50 (**1**).

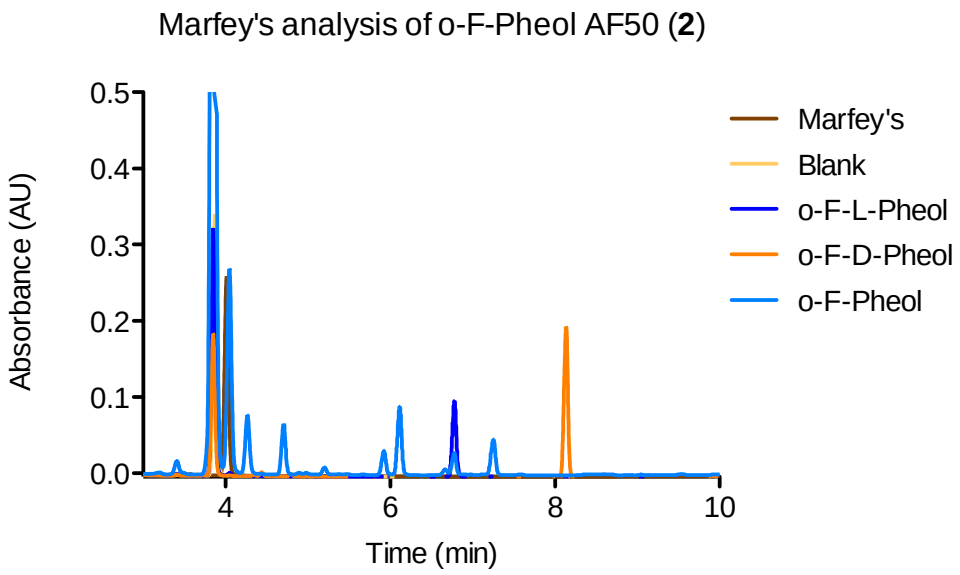

Figure S9. Marfey's analysis of *ortho*-F-Pheol alamethicin F50 (**2**).

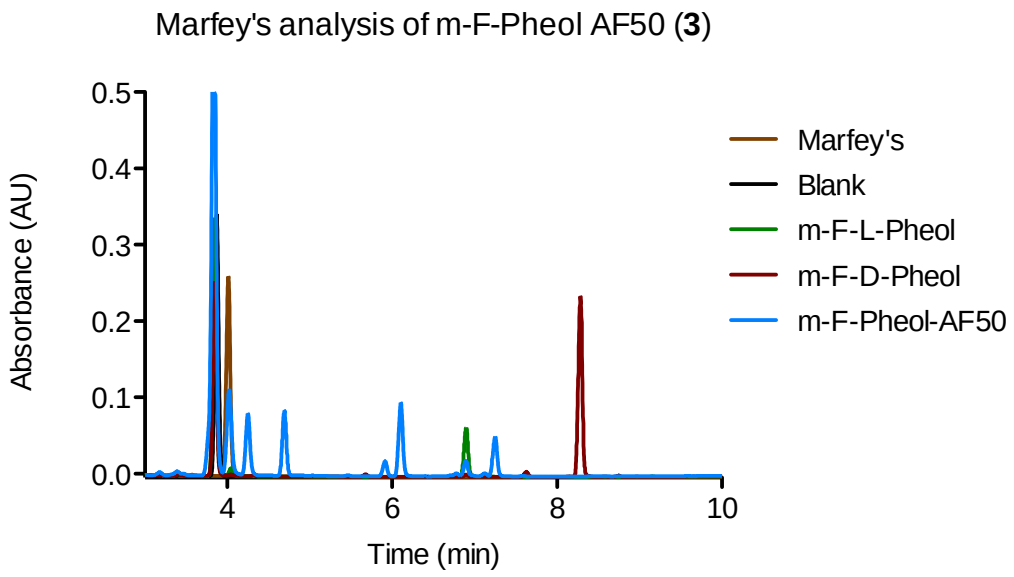

Figure S10. Marfey's analysis of *meta*-F-Pheol alamethicin F50 (**3**).

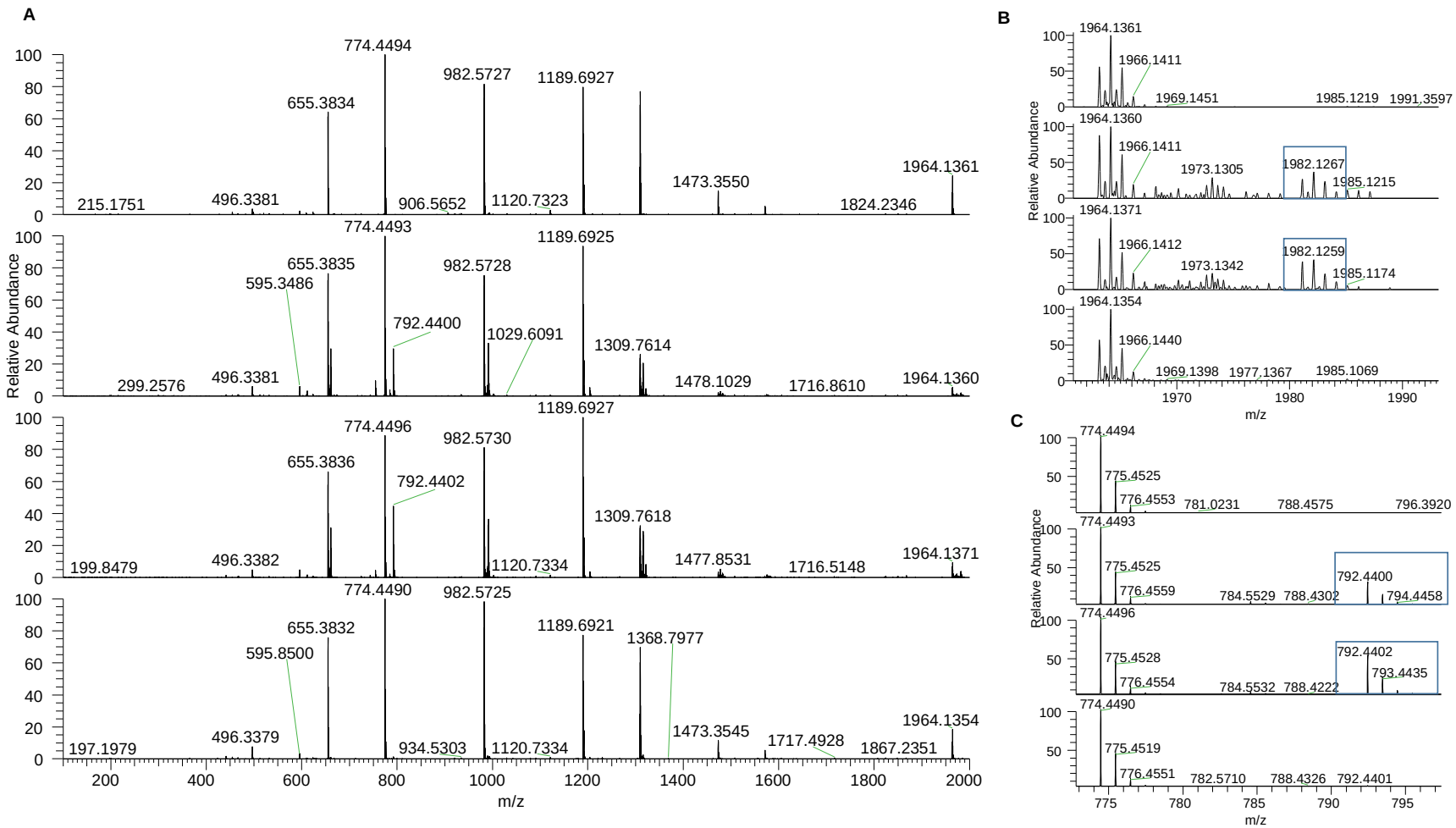

Figure S11. A) Full scan positive HRESIMS for extracts of MSX70741 cultured in rice and rice supplemented with *ortho*, *meta*, and *para*-F-DL-Phe (from the top to the bottom), indicating the incorporation of *ortho* and *meta*-F-Phe into the alamethicin F50 molecule. B) Expansion of region at *m*/*z* 1960-1990. C) Expansion of region at *m*/*z* 770-800. Diagnostic signals for the incorporation of fluorine have been boxed.

Table S3. NMR data for alamethicin F50 (**1**). Data recorded in CD_3OH. ^1H (700 MHz) and ^{13}C (175 MHz)

Compound 1 (Alamethicin F50)					
Position		**δ_C**	**δ_H, m, *J* (Hz)**	**HMBC**	**NOESY**
Ac	1	172.5			
	2	22.5	2.05, *s*	Ac-1	
Aib^1	1	175.5			
	2	57.4			
	3	23.8	1.46, *s*	Aib^1-1, Aib^1-2, Aib^1-4	
	4	26.6	1.53, *s*	Aib^1-1, Aib^1-2	
	NH		8.63, s	Ac-1, Aib^1-1, Aib^1-2	Pro^2-5a, Pro^2-5b
Pro^2	1	175.6			
	2	65.7	4.25, *t*, (8.4)	Pro^2-1, Pro^2-3	
	3	29.7^a	1.80, *m*	Pro^2-2, Pro^2-4	
			2.34, *m*	Pro^2-2, Pro^2-4	
	4	27.1	1.96, *m*	Pro^2-3, Pro^2-5	
			2.08, *m*	Pro^2-3, Pro^2-5	
	5	50.0	3.49, *td*, (9.8, 5.6)	Pro^2-4	Aib^1-NH
			3.95, *m*	Pro^2-4, Aib^1-1	Aib^1-NH
Aib^3	1	178.5			
	2	57.4			
	3	23.1	1.54, *s*	Aib^3-1, Aib^3-2	
	4	27.4	1.56, *s*	Aib^3-2	
	NH	NH	7.62, *s*	Aib^3-1, Pro^2-1	Pro^2-5a
Ala^4	1	177.2			
	2	54.1	4.09, *qd*, (7.7, 5.6)	Ala^4-1, Ala^4-3	Ala^4-NH
	3	17.1	1.49, *d*, (7.7)	Ala^4-1	
	NH		7.55, *d*, (5.6)	Ala^4-1, Aib^3-1	Ala^4-2
Aib^5	1	177.8			
	2	57.3			
	3	23.1	1.54, *s*	Aib^5-1	
	4	27.1	1.56, *s*	Aib^5-1, Aib^5-2	
	NH		7.94, *s*	Aib^5-1, Ala^4-1	Ala^4-NH (weak)
Ala^6	1	178.2			
	2	54.1	4.02, *m*	Ala^6-1, Ala^6-3	
	3	17.0	1.53, *d*, overlapped	Ala^6-2	
	NH		7.92, *brs*	Ala^6-2, Aib^5-1	Ala^6-2
Gln^7	1	175.8			
	2	58.1	3.92, *m*	Gln^7-1, Ala^6-1	
	3	27.1	2.14, *m*	Gln^7-2, Gln^7-4	
			2.27, *m*	Gln^7-2, Gln^7-4	
	4	32.6	2.34, *m*	Gln^7-2, Gln^7-3, Gln^7-5	
			2.54, *ddd*, (15.4, 9.8, 5.4)	Gln^7-2, Gln^7-3, Gln^7-5	
	5	177.3			
	NH		7.99, *d*, (4.9)	Gln^7-2, Ala^6-1	Ala^6-NH
	5-NH_2		6.77, *brs*	Gln^7-3, Gln^7-5	
			7.44, *brs*	Gln^7-5	
Aib^8	1	178.2			
	2	57.6			
	3	23.3	1.52, *s*	Aib^8-1, Aib^8-2	
	4	27.4	1.55, *s*	Aib^8-1, Aib^8-2	
	NH		8.09, s	Aib^8-1, Gln^7-1	Gln^7-2
Val^9	1	175.3			
	2	65.7	3.58, *m*	Val^9-1, Val^9-3	Aib^{10}-NH
	3	30.4	2.25, *m*	Val^9-2,	
	4	19.6	1.00, *d*, (7.0)	Val^9-2, Val^9-3	
	5	20.9	1.14, *d*, (7.0)	Val^9-2, Val^9-3	
	NH		7.49, *d*, (4.9)	Val^9-2, Aib^8-1	
Aib^{10}	1	179.0			
	2	57.6			
	3	26.8	1.54, *s*	Aib^{10}-1, Val^9-1	
	4	27.1	1.56, *s*	Aib^{10}-1, Aib^{10}-2,	
	NH		8.23, *s*	Aib^{10}-1, Val^9-1	Val^9-2, Gly^{11}-2b
Gly^{11}	1	173.0			
	2	45.1	3.66, *m*	Gly^{11}-1	
			3.93, *m*	Gly^{11}-1	
	NH		8.34, *brt*, (6.3)	Gly^{11}-2, Aib^{10}-1	Gly^{11}-2a, Gly^{11}-2b
Leu^{12}	1	175.8			
	2	54.1	4.47, *ddd*, (10.5, 7.0, 3.5)	Leu^{12}-1, Leu^{12}-3, Leu^{12}-4	
	3	41.5	1.59, overlapped	Leu^{12}-4,	
			1.96, *m*	Leu^{12}-2, Leu^{12}-4	
	4	25.7	1.91, *m*	Leu^{12}-3	
	5	21.3	0.92, *d*, (6.3)	Leu^{12}-3, Leu^{12}-4	
	6	23.4	0.94, *d*, (6.3)	Leu^{12}-3, Leu^{12}-4	
	NH		8.11, *d*, (7.7)	Leu^{12}-2, Gly^{11}-1	Gly^{11}-2a, Gly^{11}-2b
Aib^{13}	1	174.9			
	2	58.1			
	3	23.7	1.61, *s*	Aib^{13}-1, Aib^{13}-2, Aib^{13}-4	
	4	26.7	1.54, *s*	Aib^{13}-1, Aib^{13}-2	

	NH		8.41, *s*	Aib^{13}-1, Leu^{12}-1	Pro^{14}-5a, Pro^{14}-5b
Pro^{14}	1	176.4			
	2	64.7	4.39, *dd*, (9.1, 6.3)	Pro^{14}-1, Pro^{14}-3, Pro^{14}-4	
	3	30.0	1.80, *m*	Pro^{14}-2, Pro^{14}-4, Pro^{14}-5	
			2.32, *m*	Pro^{14}-2, Pro^{14}-4, Pro^{14}-5	
	4	26.9	1.99, *m*	Pro^{14}-2, Pro^{14}-3, Pro^{14}-5	
			2.08, *m*	Pro^{14}-2, Pro^{14}-3, Pro^{14}-5	
	5	50.6	3.75, *m*	Pro^{14}-3, Pro^{14}-4	
			3.87, *dt*, (11.2, 5.6)	Pro^{14}-3, Pro^{14}-4, Aib^{13}-1	Aib^{13}-NH
Val^{15}	1	175.3			
	2	64.3	3.74, *m*	Val^{15}-1, Val^{15}-3	
	3	30.5	2.34, *m*	Val^{15}-2	
	4	19.5	0.98, *d*, (7.0)	Val^{15}-2, Val^{15}-3	
	5	20.2	1.07, *d*, (7.0)	Val^{15}-2, Val^{15}-3	
	NH		7.64, *d*, (8.4)	Val^{15}-2, Pro^{14}-1	Pro^{14}-5a
Aib^{16}	1	177.6			
	2	57.6			
	3	23.4	1.54, *s*	Aib^{16}-1, Aib^{16}-2, Aib^{16}-4	
	4	27.4	1.54, *s*	Aib^{16}-1, Aib^{16}-2	
	NH		7.60, *s*	Aib^{16}-1, Aib^{16}-2, Aib^{16}-4, Val^{15}-1	Val^{15}-2
Aib^{17}	1	178.7			
	2	57.7			
	3	23.4	1.53, s	Aib^{17}-1, Aib^{17}-2	
	4	27.4	1.55, s	Aib^{17}-1, Aib^{17}-2	
	NH		7.82, *s*	Aib^{17}-1, Aib^{17}-2, Aib^{17}-3, Aib^{17}-4, Aib^{16}-1	Gln^{18}-3, Gln^{18}-4b
Gln^{18}	1	175.5			
	2	57.0	4.02, *m*	Gln^{18}-1, Aib^{17}-1	Gln^{19}-NH
	3	28.0	2.25, *m*	Gln^{18}-1, Gln^{18}-2, Gln^{18}-4	
	4	33.2	2.43, *dt*, (16.1, 8.4)	Gln^{18}-2, Gln^{18}-3, Gln^{18}-5	
			2.62, *ddd*, (15.4, 9.1, 6.3)	Gln^{18}-2, Gln^{18}-3, Gln^{18}-5	
	5	177.6			
	NH		7.79, *d*, (5.6)	Gln^{18}-2, Aib^{17}-1	
	5-NH_2		6.79, *brs*	Gln^{18}-3, ^{18}Gln^{18}-5	
			7.44, *brs*	Gln^{18}-5	
Gln^{19}	1	174.0			
	2	55.7	4.15, *m*	Gln^{19}-1, Gln^{19}-3, Gln^{18}-1	Pheol^{20}-NH
	3	28.0	2.02, *m*	Gln^{19}-2, Gln^{19}-4	
	4	32.9	2.20, *m*	Gln^{19}-2, ^{19}Gln^{19}-3, Gln^{19}-5	
			2.34, *m*	Gln^{19}-2, ^{19}Gln^{19}-3, Gln^{19}-5	
	5	177.3			
	NH		7.88, *d*, (7.0)	Gln^{19}-2, Gln^{18}-1	Pheol^{20}-2
	5-NH_2		6.63, *brs*	Gln^{19}-3, Gln^{19}-5	
			7.34, *brs*	Gln^{19}-5	
Pheol^{20}	1	64.9	3.61, *brs*	Pheol^{20}-3	
	2	54.5	4.15, *m*	Pheol^{20}-3	Gln^{19}-NH
	3	38.0	2.73, *dd*, (14.0, 9.1)	Pheol^{20}-1, Pheol^{20}-2 Pheol^{20}-4, Pheol^{20}-5	
			2.94, *dd*, (14.0, 5.6)	Pheol^{20}-1, Pheol^{20}-2 Pheol^{20}-4, Pheol^{20}-5	
	4	139.8			
	5	130.4	7.28, *d*, (7.7)	Pheol^{20}-7, Pheol^{20}-9	
	6	129.1	7.22, *t* (7.7)	Pheol^{20}-4, Pheol^{20}-5, Pheol^{20}-8	
	7	127.1	7.14, *t*, (7.7)	Pheol^{20}-5, Pheol^{20}-9	
	8	129.1	7.22, *t* (7.7)	Pheol^{20}-4, Pheol^{20}-5, Pheol^{20}-6	
	9	130.4	7.28, *d*, (7.7)	Pheol^{20}-5, Pheol^{20}-7	
	NH		7.32, *d*, (9.1)	Pheol^{20}-2, Gln^{19}-1	Pheol^{20}-1, Pheol^{20}-2

[a]Signals may be exchangeable

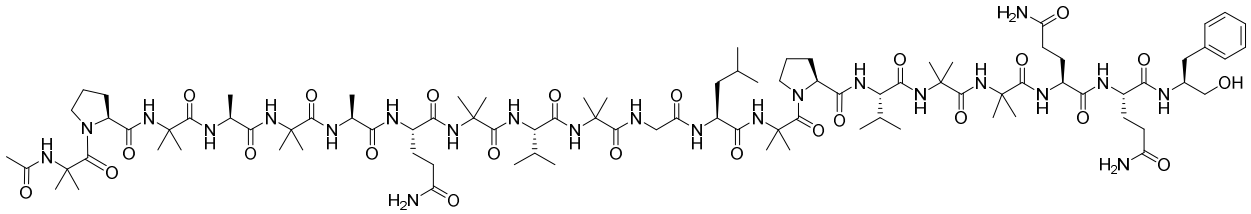

Alamethicin F50 (**1**)

Table S4. NMR data for *ortho*-F-Pheol alamethicin F50 (**2**). Data recorded in CD_3OH. ^{1}H (700 MHz), ^{13}C (175 MHz), and ^{19}F (470 MHz)

Compound 2 (*ortho*-F-Pheol-alamethicin F50)					
Position		**δ_C**	**δ_H, m, *J* (Hz)**	**HMBC**	**NOESY**
Ac	1	172.5			
	2	22.4	2.05, *s*	Ac-1	
Aib^{1}	1	175.5			
	2	57.4			
	3	23.8	1.46, *s*	Aib^{1}-1, Aib^{1}-2, Aib^{1}-4	
	4	26.6	1.53, *s*	Aib^{1}-1, Aib^{1}-2	
	NH		8.63, s	Ac-1, Aib^{1}-1, Aib^{1}-2	Pro^{2}-5a, Pro^{2}-5b
Pro^{2}	1	175.6			
	2	65.7	4.25, *t* (8.4)	Pro^{2}-1, Pro^{2}-3	
	3	29.7	1.80, *m*	Pro^{2}-2, Pro^{2}-4	
			2.34, *m*	Pro^{2}-2, Pro^{2}-4	
	4	27.1^{a}	1.97, *m*	Pro^{2}-3, Pro^{2}-5	
			2.08, *m*	Pro^{2}-3, Pro^{2}-5	
	5	49.9	3.48, *td*, (10.5, 6.3)	Pro^{2}-4	Aib^{1}-NH
			3.95, *m*	Pro^{2}-4, Aib^{1}-1	Aib^{1}-NH
Aib^{3}	1	178.5			
	2	57.4			
	3	23.1	1.54, *s*	Aib^{3}-1, Aib^{3}-2	
	4	27.4	1.56, *s*	Aib^{3}-2	
	NH	NH	7.62, *s*	Aib^{3}-1, Pro^{2}-1	Pro^{2}-5a
Ala^{4}	1	177.2			
	2	54.1	4.09, *m*	Ala^{4}-1, Ala^{4}-3	Ala^{4}-NH
	3	17.1	1.48, *d*, (7.7)	Ala^{4}-2	
	NH		7.56, *d*, (5.6)	Ala^{4}-1	Ala^{4}-2
Aib^{5}	1	177.8			
	2	57.3			
	3	23.1	1.54, *s*	Aib^{5}-1	
	4	27.1	1.56, *s*	Aib^{5}-1, Aib^{5}-2	
	NH		7.93, *s*	Aib^{5}-1, Ala^{4}-1	Ala^{4}-NH
Ala^{6}	1	178.1			
	2	53.9	4.02, *m*	Ala^{6}-1, Ala^{6}-3	
	3	16.9	1.53, *d*, overlapped	Ala^{6}-2	
	NH		7.92, *brs*	Ala^{6}-2	Ala^{6}-2
Gln^{7}	1	175.8			
	2	58.1	3.94, *m*	Gln^{7}-1, Ala^{6}-1	
	3	27.1	2.15, *m*	Gln^{7}-2, Gln^{7}-4	
			2.30, *m*	Gln^{7}-2, Gln^{7}-4	
	4	32.6	2.34, *m*	Gln^{7}-2, Gln^{7}-3, Gln^{7}-5	
			2.54, *ddd*, (15.4, 9.8, 5.6)	Gln^{7}-2, Gln^{7}-3, Gln^{7}-5	
	5	177.3			
	NH		8.00, *d*, (5.6)	Gln^{7}-2, Ala^{6}-1	Ala^{6}-NH
	5-NH_2		6.77, *brs*	Gln^{7}-3, Gln^{7}-5	
			7.44, *brs*	Gln^{7}-5	
Aib^{8}	1	178.2			
	2	57.6			
	3	23.3	1.52, *s*	Aib^{8}-1, Aib^{8}-2	
	4	27.4	1.55, *s*	Aib^{8}-1, Aib^{8}-2	
	NH		8.09, s	Aib^{8}-1, Gln^{7}-1	Gln^{7}-2
Val^{9}	1	175.3			
	2	65.7	3.58, *dd*, (9.8, 3.5)	Val^{9}-1, Val^{9}-3	Aib^{10}-NH
	3	30.4	2.25, *m*	Val^{9}-2,	
	4	19.6	1.00, *d*, (6.3)	Val^{9}-2, Val^{9}-3	
	5	20.8	1.13, *d*, (6.3)	Val^{9}-2, Val^{9}-3	
	NH		7.49, *d*, (4.9)	Val^{9}-2, Aib^{8}-1	
Aib^{10}	1	179.0			
	2	57.6			
	3	26.8	1.54, *s*	Aib^{10}-1, Val^{9}-1	
	4	27.1	1.56, *s*	Aib^{10}-1, Aib^{10}-2,	
	NH		8.22, *s*		Val^{9}-2, Gly^{11}-2b
Gly^{11}	1	173.0			
	2	45.1	3.67, *m*	Gly^{11}-1	
			3.94, *m*	Gly^{11}-2, Aib^{10}-1	
	NH		8.34, *brt*, (5.6)	Gly^{11}-1, Aib^{10}-1	Gly^{11}-2a, Gly^{11}-2b
Leu^{12}	1	175.8			
	2	54.1	4.46, *m*	Leu^{12}-1, Leu^{12}-3, Leu^{12}-4	
	3	41.5	1.59, overlapped	Leu^{12}-4,	
			1.96, *m*	Leu^{12}-2, Leu^{12}-4	
	4	25.6	1.91, *m*	Leu^{12}-3	
	5	21.3	0.92, *d*, (6.3)	Leu^{12}-3, Leu^{12}-4	
	6	23.4	0.94, *d*, (6.3)	Leu^{12}-3, Leu^{12}-4	
	NH		8.11, *d*, (8.4)	Leu^{12}-2, Gly^{11}-1	Gly^{11}-2a, Gly^{11}-2b
Aib^{13}	1	174.9			
	2	58.1			
	3	23.7	1.61, *s*	Aib^{13}-1, Aib^{13}-2, Aib^{13}-4	

	4	26.7	1.54, *s*	Aib^{13}-1, Aib^{13}-2	
	NH		8.40, *s*	Aib^{13}-1, Leu^{12}-1	Pro^{14}-5a, Pro^{14}-5b
Pro^{14}	1	176.4			
	2	64.6	4.38, *dd*, (9.1, 6.3)	Pro^{14}-1, Pro^{14}-3, Pro^{14}-4	
	3	30.0	1.80, *m*	Pro^{14}-2, Pro^{14}-4, Pro^{14}-5	
			2.35, *m*	Pro^{14}-2, Pro^{14}-4, Pro^{14}-5	
	4	26.9[a]	1.99, *m*	Pro^{14}-2, Pro^{14}-3, Pro^{14}-5	
			2.08, *m*	Pro^{14}-2, Pro^{14}-3, Pro^{14}-5	
	5	50.6	3.73, *m*	Pro^{14}-3, Pro^{14}-4	
			3.88, *dt*, (11.2, 6.3)	Pro^{14}-3, Pro^{14}-4, Aib^{13}-1	Aib^{13}-NH
Val^{15}	1	175.3			
	2	64.3	3.73, *m*	Val^{15}-1, Val^{15}-3	
	3	30.5	2.34, *m*	Va^{15}-2	
	4	19.4	0.97, *d*, (6.3)	Val^{15}-2, Val^{15}-3	
	5	20.2	1.07, *d*, (6.3)	Val^{15}-2, Val^{15}-3	
	NH		7.63, *d*, overlapped	Val^{15}-2, Pro^{14}-1	Pro^{14}-5a
Aib^{16}	1	177.6			
	2	57.6			
	3	23.4	1.54, *s*	Aib^{16}-1, Aib^{16}-2, Aib^{16}-4	
	4	27.4	1.54, *s*	Aib^{16}-1, Aib^{16}-2	
	NH		7.58, *s*	Aib^{16}-1, Aib^{16}-2, Aib^{16}-4, Val^{15}-1	Val^{15}-2
Aib^{17}	1	178.8			
	2	57.7			
	3	23.4	1.53, s	Aib^{17}-1, Aib^{17}-2	
	4	27.4	1.55, s	Aib^{17}-1, Aib^{17}-2	
	NH		7.81, *s*	Aib^{17}-1, Aib^{17}-2, Aib^{17}-3, Aib^{16}-1	Gln^{18}-3, Gln^{18}-4b
Gln^{18}	1	175.6			
	2	57.0	4.01, *m*	Gln^{18}-1, Aib^{17}-1	Gln^{19}-NH
	3	28.0	2.25, *m*	Gln^{18}-1, Gln^{18}-2, Gln^{18}-4	
	4	33.2	2.43, *dt*, (15.4, 8.4)	Gln^{18}-2, Gln^{18}-3, Gln^{18}-5	
			2.62, *dt*, (15.4, 7.7)	Gln^{18}-2, Gln^{18}-3, Gln^{18}-5	
	5	177.4			
	NH		7.78, *d*, (5.6)	Gln^{18}-2, Aib^{17}-1	
	5-NH$_2$		6.78, *brs*	Gln^{18}-3, Gln^{18}-5	
			7.44, *brs*	Gln^{18}-5	
Gln^{19}	1	174.1			
	2	55.7	4.15, *m*	Gln^{19}-1, Gln^{19}-3, Gln^{18}-1	Pheol^{20}-NH
	3	27.9	1.99, *m*	Gln^{19}-2, Gln^{19}-4	
	4	32.9	2.19, *m*	Gln^{19}-2, Gln^{19}-3, Gln^{19}-5	
			2.34, *m*	Gln^{19}-2, Gln^{19}-3, Gln^{19}-5	
	5	177.3			
	NH		7.86, *d*, (7.7)	Gln^{19}-2, Gln^{18}-1	Pheol^{20}-2
	5-NH$_2$		6.62, *brs*	Gln^{19}-3, Gln^{19}-5	
			7.35, *brs*	Gln^{19}-5	
F-Pheol^{20}	1	65.1	3.65, *brt*	F-Pheol^{20}-3	
	2	52.9	4.25, *m*	F-Pheol^{20}-3	Gln^{19}-NH
	3	31.1	2.70, *dd*, (14.0, 9.1)	F-Pheol^{20}-1, F-Pheol^{20}-2, F-Pheol^{20}-4, F-Pheol^{20}-5	
			3.07, *dd*, (14.0, 4.9)	F-Pheol^{20}-1, F-Pheol^{20}-2, F-Pheol^{20}-4, F-Pheol^{20}-5	
	4	126.5, *d*, (15.4)			
	5	162.6, *d*, (242.7)			
	6	115.5, *d*, (22.1)	6.99, *t*, (9.1)	F-Pheol^{20}-4, F-Pheol^{20}-5, F-Pheol^{20}-8	
	7	129.1, *d*, (8.4)	7.18, *dd*, (7.1, 7.0)	F-Pheol^{20}-5, F-Pheol^{20}-9	
	8	124.9, *d*, (3.7)	7.04, *t*, (7.7)	F-Pheol^{20}-4, F-Pheol^{20}-6	
	9	132.9, *d*, (4.4)	7.37, *t*, (7.7)	F-Pheol^{20}-5, F-Pheol^{20}-7	
	1-OH		5.23, *t*, (6.6)		
	NH		7.32, *d*, (9.1)	Gln^{19}-1	F-Pheol^{20}-1, F-Pheol^{20}-2
	F		-119.7*, *m*		

*Recorded at 470 MHz

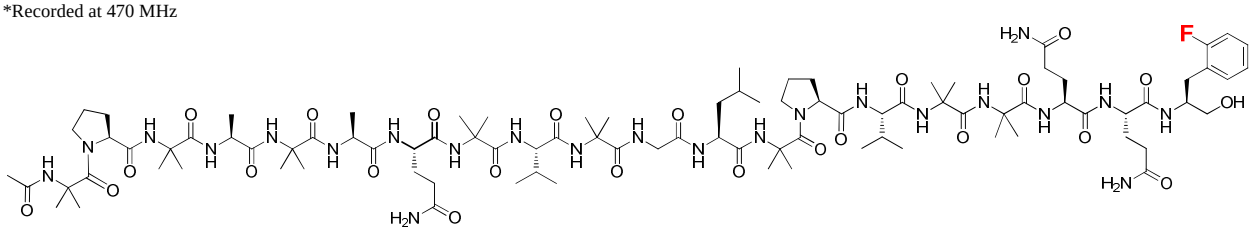

ortho-F-Pheol alamethicin F50 (**2**)

Table S5. NMR data for *meta*-F-Pheol alamethicin F50 (**3**). Data recorded in CD_3OH. ^1H (700 MHz), ^{13}C (175 MHz), and ^{19}F (470 MHz)

Compound 3 (*meta*-F-Pheol-alamethicin F50)					
residue	**position**	**δ_C**	**δ_H, m, *J* (Hz)**	**HMBC**	**NOESY**
Ac	1	172.5			
	2	22.4	2.05, *s*	Ac-1	
Aib^1	1	175.5			
	2	57.4			
	3	23.8	1.46, *s*	Aib^1-1, Aib^1-2, Aib^1-4	
	4	26.6	1.54, *s*	Aib^1-1, Aib^1-2	
	NH		8.64, s	Ac-1, Aib^1-1, Aib^1-2	Pro^2-5a, Pro^2-5b
Pro^2	1	175.6			
	2	65.7	4.25, *t* (8.4)	Pro^2-1, Pro^2-3	
	3	29.7	1.80, *m*	Pro^2-2, Pro^2-4	
			2.34, *m*	Pro^2-2, Pro^2-4	
	4	27.1^a	1.97, *m*	Pro^2-3, Pro^2-5	
			2.08, *m*	Pro^2-3, Pro^2-5	
	5	49.9	3.49, *td*, (10.5, 6.3,)	Pro^2-4	Aib^1-NH
			3.95, *m*	Pro^2-4, Aib^1-1	Aib^1-NH
Aib^3	1	178.5			
	2	57.4			
	3	23.1	1.54, *s*	Aib^3-1, Aib^3-2	
	4	27.4	1.56, *s*	Aib^3-2	
	NH	NH	7.62, *s*	Aib^3-1, Pro^2-1	Pro^2-5a
Ala^4	1	177.2			
	2	54.1	4.09, *m*	Ala^4-1, Ala^4-3	Ala^4-NH
	3	17.0	1.48, *d*, (7.7)	Ala^4-2	
	NH		7.56, *d*, (4.2)	Ala^4-1	Ala^4-2
Aib^5	1	177.8			
	2	57.3			
	3	23.1	1.54, *s*	Aib^5-1	
	4	27.1	1.56, *s*	Aib^5-1, Aib^5-2	
	NH		7.93, *s*	Aib^5-1, Ala^4-1	Ala^4-NH
Ala^6	1	178.1			
	2	53.8	4.01, *m*	Ala^6-1, Ala^6-3	
	3	16.9	1.53, *d*, overlapped	Ala^6-2	
	NH		7.91, *brs*	Ala^6-2	Ala^6-2
Gln^7	1	175.8			
	2	58.1	3.94, *m*	Gln^7-1, Ala^6-1	
	3	27.3	2.15, *m*	Gln^7-2, Gln^7-4	
			2.30, *m*	Gln^7-2, Gln^7-4	
	4	32.5	2.34, *m*	Gln^7-2, Gln^7-3, Gln^7-5	
			2.54, *ddd*, (15.4, 9.8, 6.3)	Gln^7-2, Gln^7-3, Gln^7-5	
	5	177.1			
	NH		7.99, *d*, (4.9)	Gln^7-2, Ala^6-1	Ala^6-NH
	5-NH_2		6.77, *brs*	Gln^7-3, Gln^7-5	
			7.45, *brs*	Gln^7-5	
Aib^8	1	178.2			
	2	57.6			
	3	23.3	1.52, *s*	Aib^8-1, Aib^8-2	
	4	27.4	1.55, *s*	Aib^8-1, Aib^8-2	
	NH		8.08, s	Aib^8-1, Gln^7-1	Gln^7-2
Val^9	1	175.3			
	2	65.7	3.58, *dd*, (9.3, 3.2)	Val^9-1, Val^9-3	Aib^{10}-NH
	3	30.6	2.25, *m*	Val^9-2,	
	4	19.6	1.00, *d*, (6.4)	Val^9-2, Val^9-3	
	5	20.8	1.13, *d*, (6.3)	Val^9-2, Val^9-3	
	NH		7.49, *d*, (4.9)	Val^9-2, Aib^8-1	
Aib^{10}	1	179.0			
	2	57.6			
	3	26.8	1.54, *s*	Aib^{10}-1, Val^9-1	
	4	27.1	1.56, *s*	Aib^{10}-1, Aib^{10}-2,	
	NH		8.22, *s*		Val^9-2, Gly^{11}-2b
Gly^{11}	1	173.0		Gly^{11}-1	
	2	45.0	3.67, *dd* (16.8, 5.6)	Gly^{11}-1	
			3.95, *m*	Gly^{11}-2, Aib^{10}-1	
	NH		8.34, *brt*, (5.7)	Gly^{11}-1, Aib^{10}-1	Gly^{11}-2a, Gly^{11}-2b
Leu^{12}	1	175.8			
	2	54.0	4.45, *m*	Leu^{12}-1, Leu^{12}-3, Leu^{12}-4	
	3	41.5	1.59, overlapped	Leu^{12}-4,	
			1.96, *m*	Leu^{12}-2, Leu^{12}-4	
	4	25.6	1.91, *m*	Leu^{12}-3	
	5	21.3	0.92, *d*, (6.3)	Leu^{12}-3, Leu^{12}-4	
	6	23.4	0.94, *d*, (6.3)	Leu^{12}-3, Leu^{12}-4	
	NH		8.11, *d*, (7.8)	Leu^{12}-2, Gly^{11}-1	Gly^{11}-2a, Gly^{11}-2b
Aib^{13}	1	174.9			
	2	58.1			
	3	23.7	1.61, *s*	Aib^{13}-1, Aib^{13}-2, Aib^{13}-4	

	4	26.6	1.54, *s*	Aib^{13}-1, Aib^{13}-2	
	NH		8.40, *s*	Aib^{13}-1, Leu^{12}-1	Pro^{14}-5a, Pro^{14}-5b
Pro^{14}	1	176.4			
	2	64.6	4.39, *dd*, (8.9, 6.5)	Pro^{14}-1, Pro^{14}-3, Pro^{14}-4	
	3	30.0	1.80, *m*	Pro^{14}-2, Pro^{14}-4, Pro^{14}-5	
			2.35, *m*	Pro^{14}-2, Pro^{14}-4, Pro^{14}-5	
	4	26.9^{a}	1.99, *m*	Pro^{14}-2, Pro^{14}-3, Pro^{14}-5	
			2.08, *m*	Pro^{14}-2, Pro^{14}-3, Pro^{14}-5	
	5	50.5	3.73, *m*	Pro^{14}-3, Pro^{14}-4	
			3.88, *dt*, (11.9, 6.2)	Pro^{14}-3, Pro^{14}-4, Aib^{13}-1	Aib^{13}-NH
Val^{15}	1	175.3			
	2	64.3	3.73, *m*	Val^{15}-1, Val^{15}-3	
	3	30.5	2.34, *m*	Va^{15}-2	
	4	19.4	0.98, *d*, (6.5)	Val^{15}-2, Val^{15}-3	
	5	20.2	1.07, *d*, (6.4)	Val^{15}-2, Val^{15}-3	
	NH		7.63, *d* (8.0)	Val^{15}-2, Pro^{14}-1	Pro^{14}-5a
Aib^{16}	1	177.6			
	2	57.6			
	3	23.4	1.54, *s*	Aib^{16}-1, Aib^{16}-2, Aib^{16}-4	
	4	27.4	1.54, *s*	Aib^{16}-1, Aib^{16}-2	
	NH		7.59, *s*	Aib^{16}-1, Aib^{16}-2, Aib^{16}-4, Val^{15}-1	Val^{15}-2
Aib^{17}	1	178.8			
	2	57.7			
	3	23.4	1.53, s	Aib^{17}-1, Aib^{17}-2	
	4	27.4	1.55, s	Aib^{17}-1, Aib^{17}-2	
	NH		7.81, *s*	Aib^{17}-1, Aib^{17}-2, Aib^{17}-3, Aib^{16}-1	Gln^{18}-3, Gln^{18}-4b
Gln^{18}	1	175.5			
	2	57.0	4.01, *m*	Gln^{18}-1, Aib^{17}-1	Gln^{19}-NH
	3	28.0	2.25, *m*	Gln^{18}-1, Gln^{18}-2, Gln^{18}-4	
	4	33.1	2.43, *dt*, (15.5, 8.6)	Gln^{18}-2, Gln^{18}-3, Gln^{18}-5	
			2.62, *dt*, (15.2, 8.0)	Gln^{18}-2, Gln^{18}-3, Gln^{18}-5	
	5	177.4			
	NH		7.79, *d*, (5.4)	Gln^{18}-2, Aib^{17}-1	
	5-NH$_2$		6.79, *brs*	Gln^{18}-3, Gln^{18}-5	
			7.45, *brs*	Gln^{18}-5	
Gln^{19}	1	174.0			
	2	55.6	4.16, *m*	Gln^{19}-1, Gln^{19}-3, Gln^{18}-1	Pheol^{20}-NH
	3	27.9	2.01-2.05, *m*	Gln^{19}-2, Gln^{19}-4	
	4	32.9	2.23, *m*	Gln^{19}-2, Gln^{19}-3, Gln^{19}-5	
			2.34, *m*	Gln^{19}-2, Gln^{19}-3, Gln^{19}-5	
	5	177.3			
	NH		7.87, *d*, (7.5)	Gln^{19}-2, Gln^{18}-1	Pheol^{20}-2
	5-NH$_2$		6.63, *brs*	Gln^{19}-3, Gln^{19}-5	
			7.35, *brs*	Gln^{19}-5	
F-Pheol^{20}	1	64.9	3.63, *brt*	F-Pheol^{20}-3	
	2	54.0	4.16, *m*	F-Pheol^{20}-3	Gln^{19}-NH
	3	37.7	2.72, *dd*, (14.2, 9.7,)	F-Pheol^{20}-1, F-Pheol^{20}-2, F-Pheol^{20}-4, F-Pheol^{20}-5	
			2.98, *dd*, (13.9, 4.8)	F-Pheol^{20}-1, F-Pheol^{20}-2, F-Pheol^{20}-4, F-Pheol^{20}-5	
	4	142.6, *d*, (7.4)			
	5	117.1, *d*, (21.0)	7.06, *brd* (10.2)	F-Pheol^{20}-4	
	6	160.0, *d*, (242.4)			
	7	113.8, *d*, (21.0)	6.88, *td*, (8.5, 2.3)	F-Pheol^{20}-5, F-Pheol^{20}-6, F-Pheol^{20}-9	
	8	130.7, *d*, (8.2)	7.24, *t*, (7.6)	F-Pheol^{20}-4, F-Pheol^{20}-6	
	9	126.3, *d*, (2.6)	7.10, *d*, (7.6)	F-Pheol^{20}-5, F-Pheol^{20}-7	
	1-OH		5.27, *t*, (6.6)		
	NH		7.22, *d*, overlapped	Gln^{19}-1	F-Pheol^{20}-1, F-Pheol^{20}-2
	F		-115.8*, *m*		

*Recorded at 470 MHz

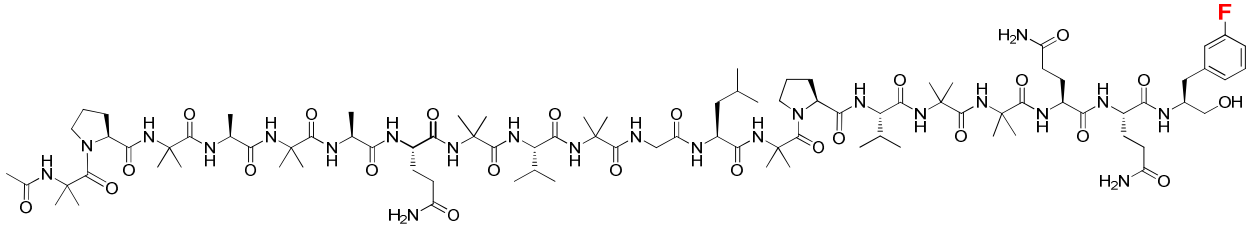

meta-F-Pheol alamethicin F50 (**3**)

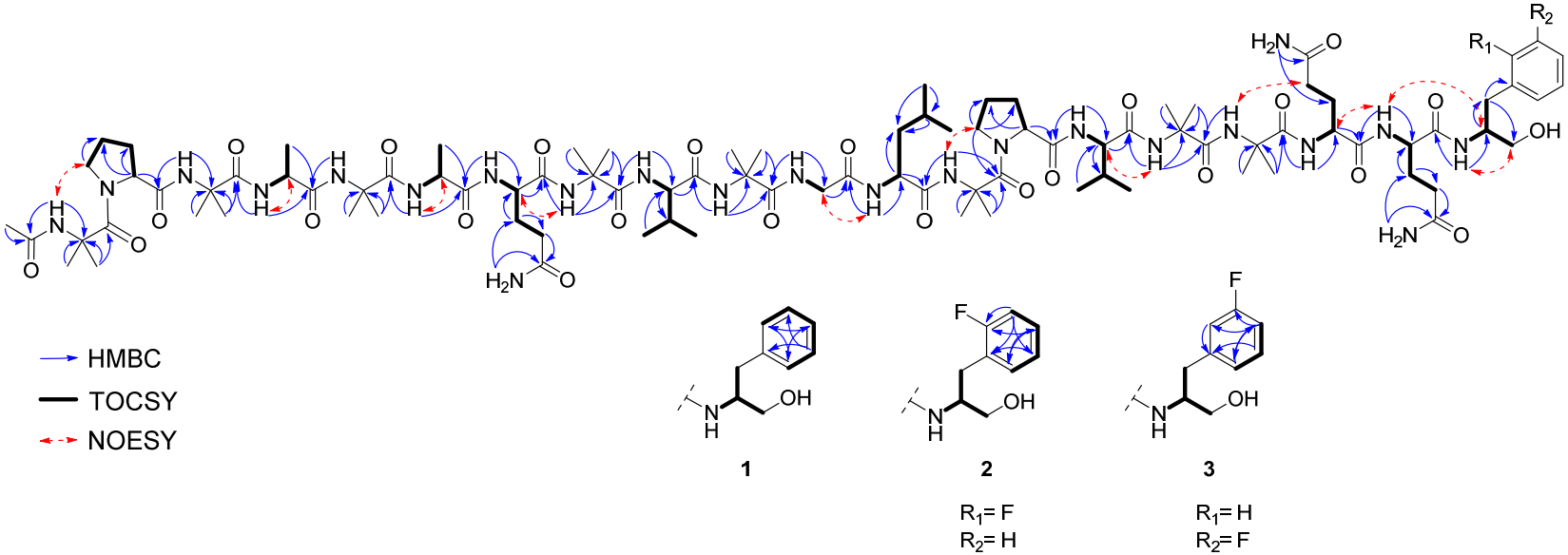

Figure S12. Key HMBC, TOCSY and NOESY correlations for compounds **1-3**.

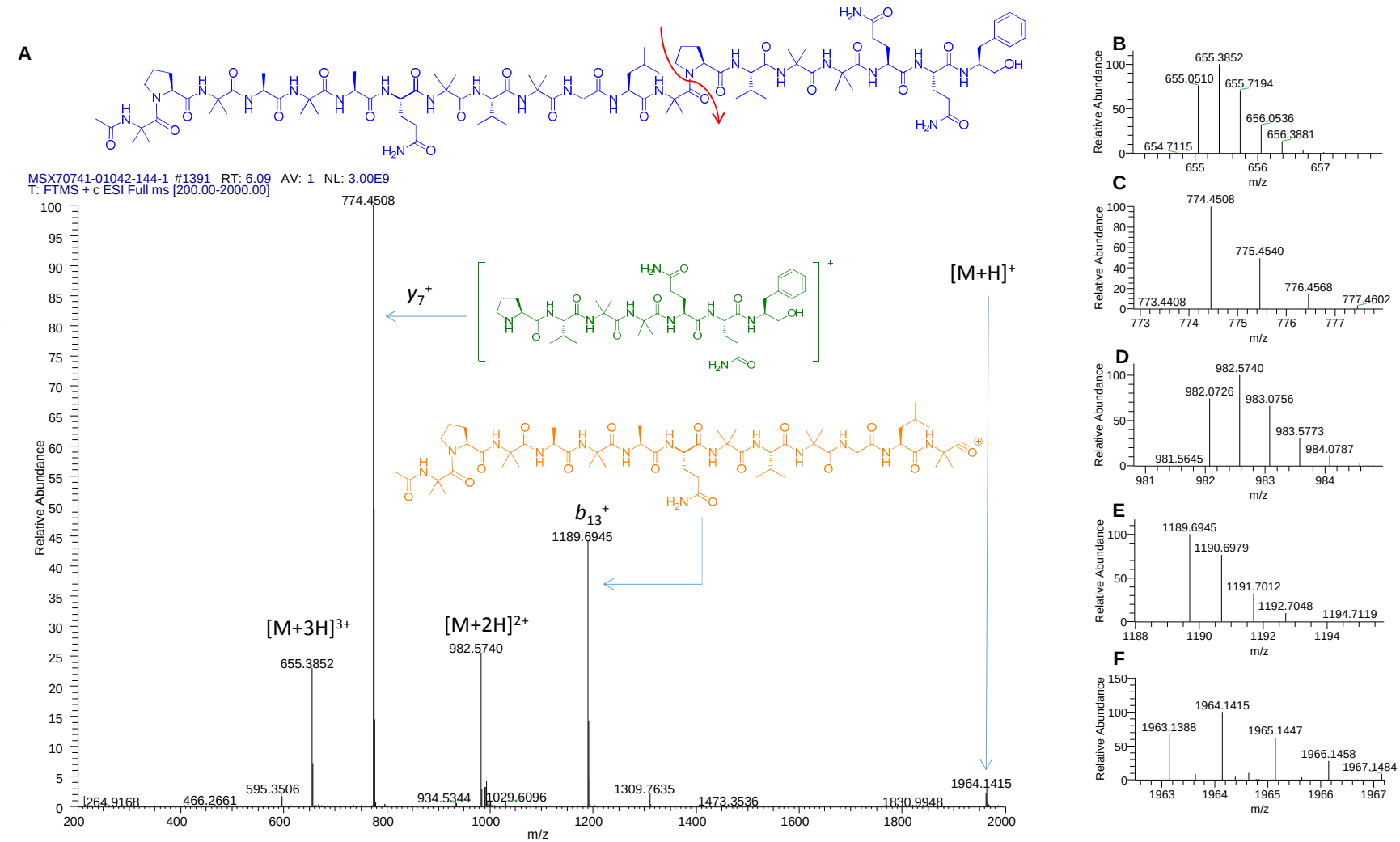

Figure S13. A) Full scan positive HRESIMS for compound **1**. B-F) Expansion of the $[M+3H]^{3+}$, y_7^+, $[M+2H]^{2+}$, b_{13}^+, and $[M+H]^+$ ion peaks, respectively.

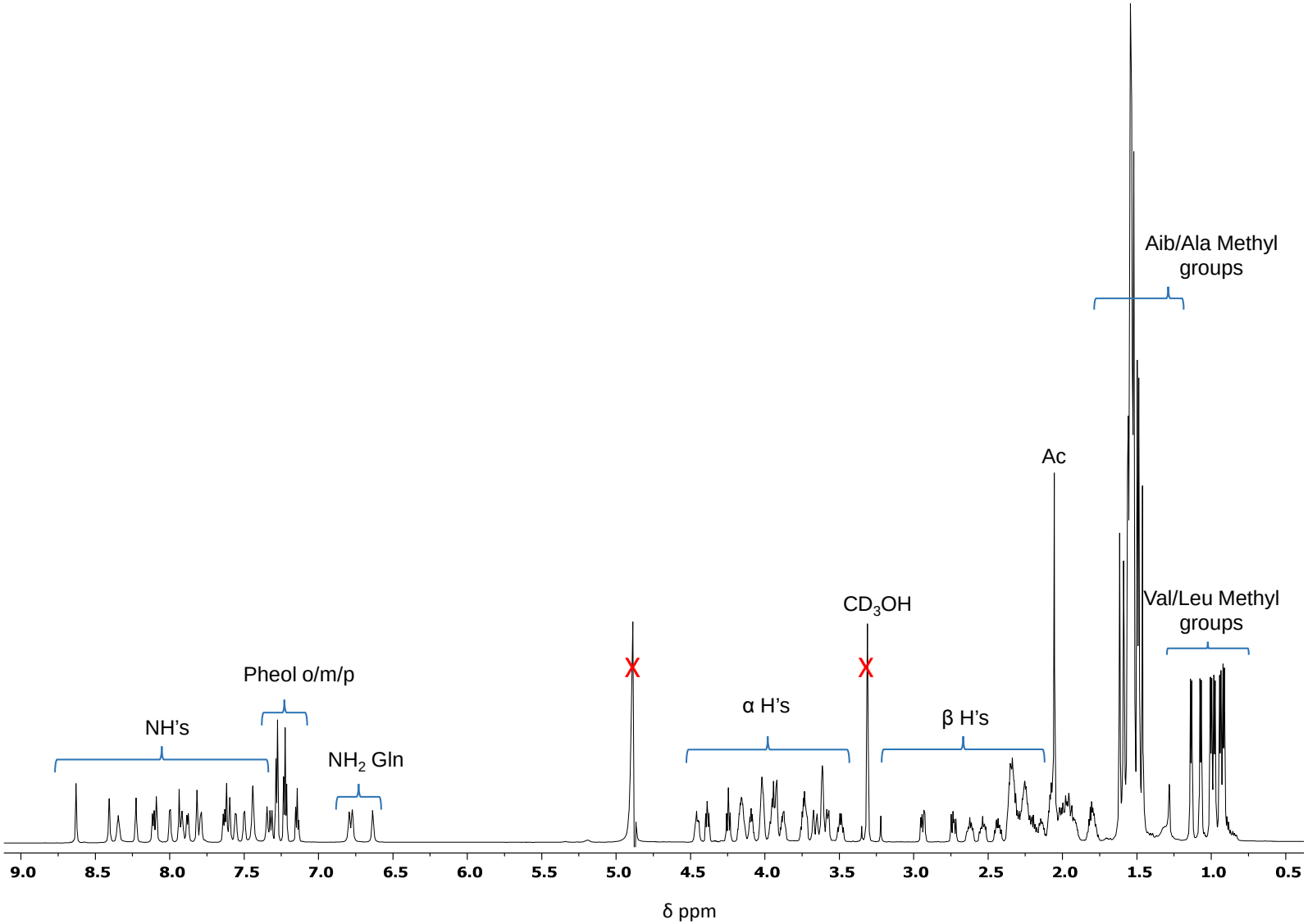

Figure S14. ^{1}H-NMR spectrum of alamethicin F50 (**1**) in CD_3OH (recorded at 700 MHz).

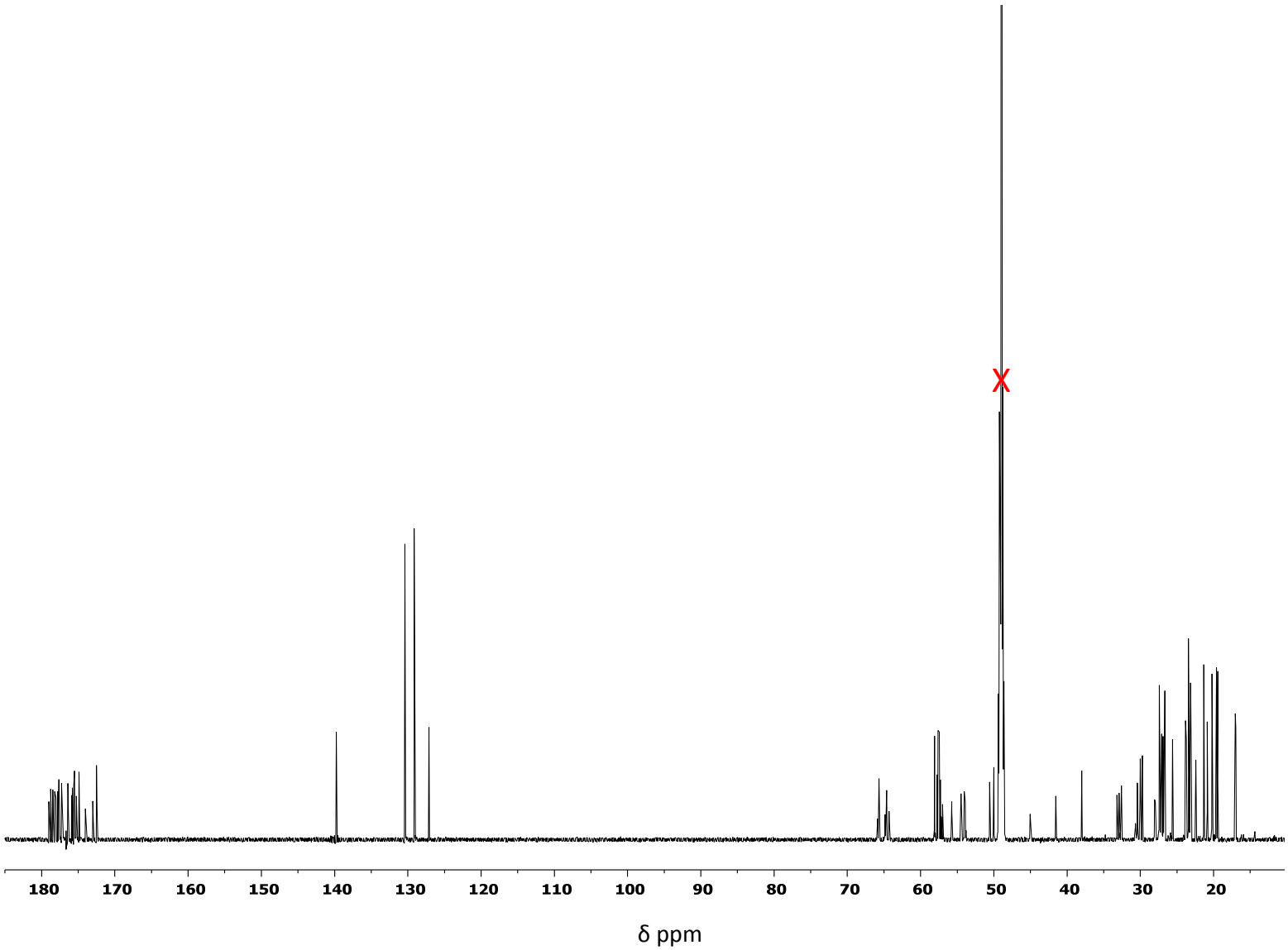

Figure S15. ^{13}C-NMR spectrum of alamethicin F50 (**1**) in CD_3OH (recorded at 175 MHz).

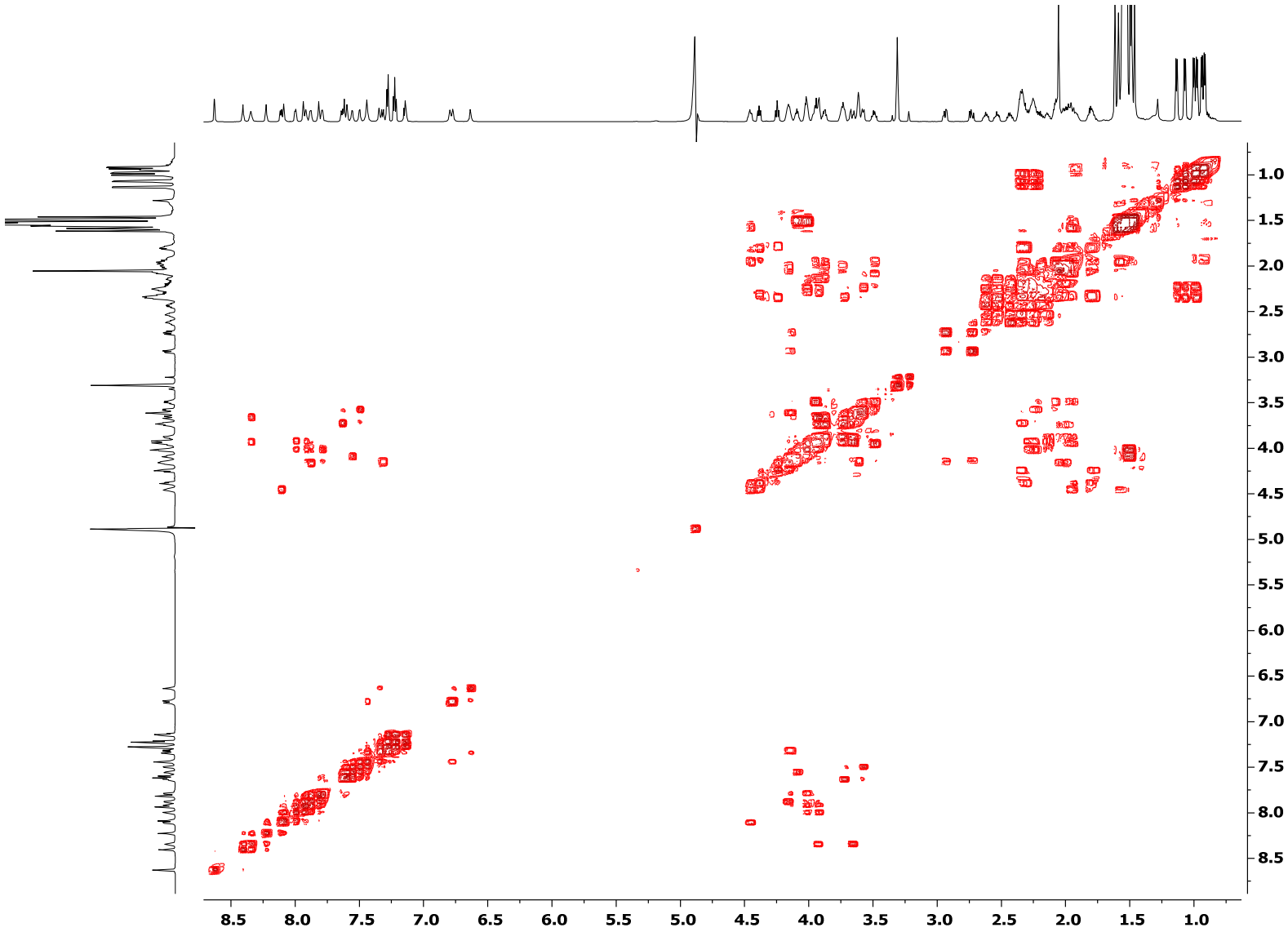

Figure S16. ^{1}H-^{1}H COSY of alamethicin F50 (**1**) in CD_3OH.

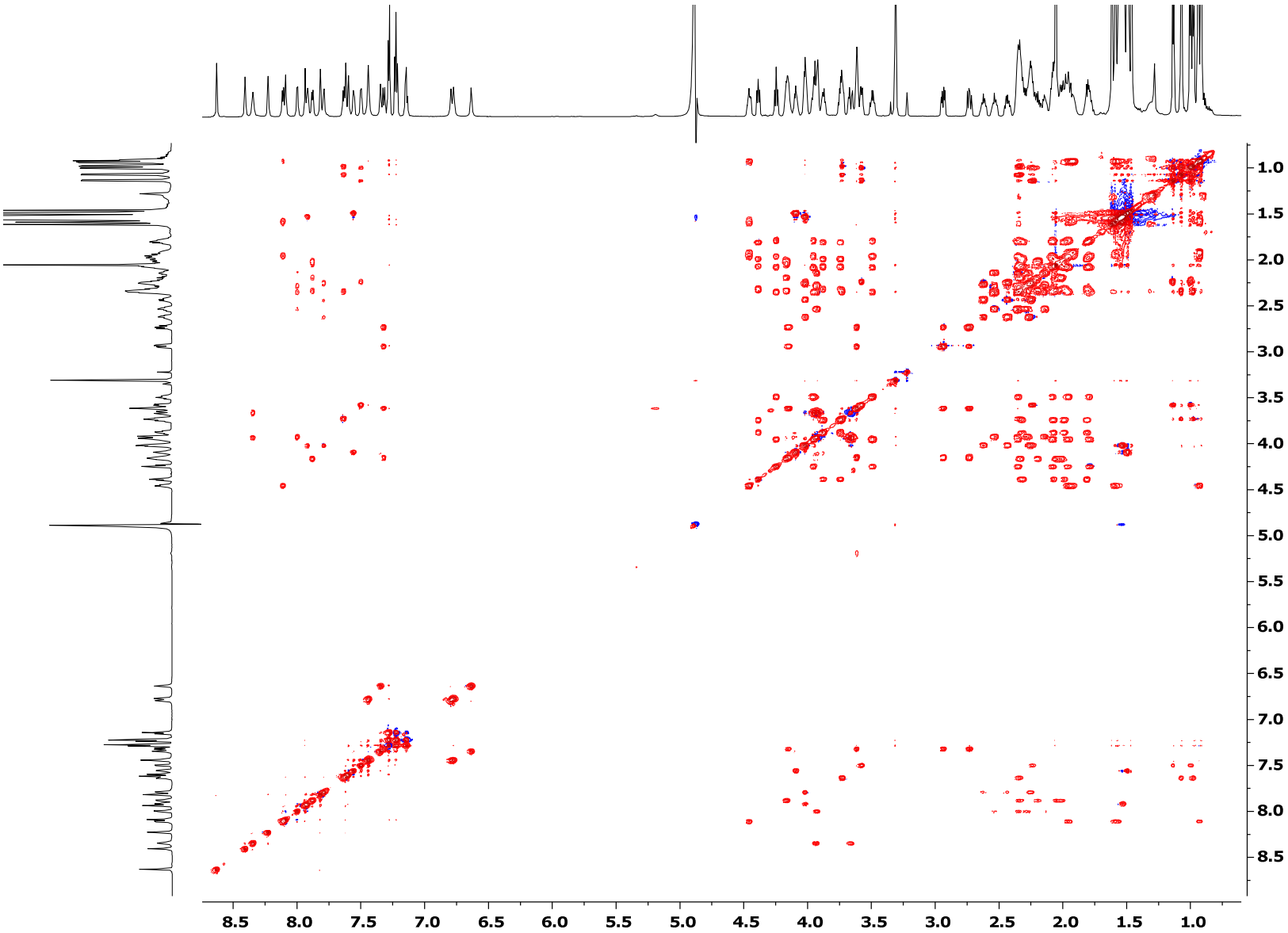

Figure S17. ^{1}H-^{1}H TOCSY of alamethicin F50 (**1**) in CD_3OH.

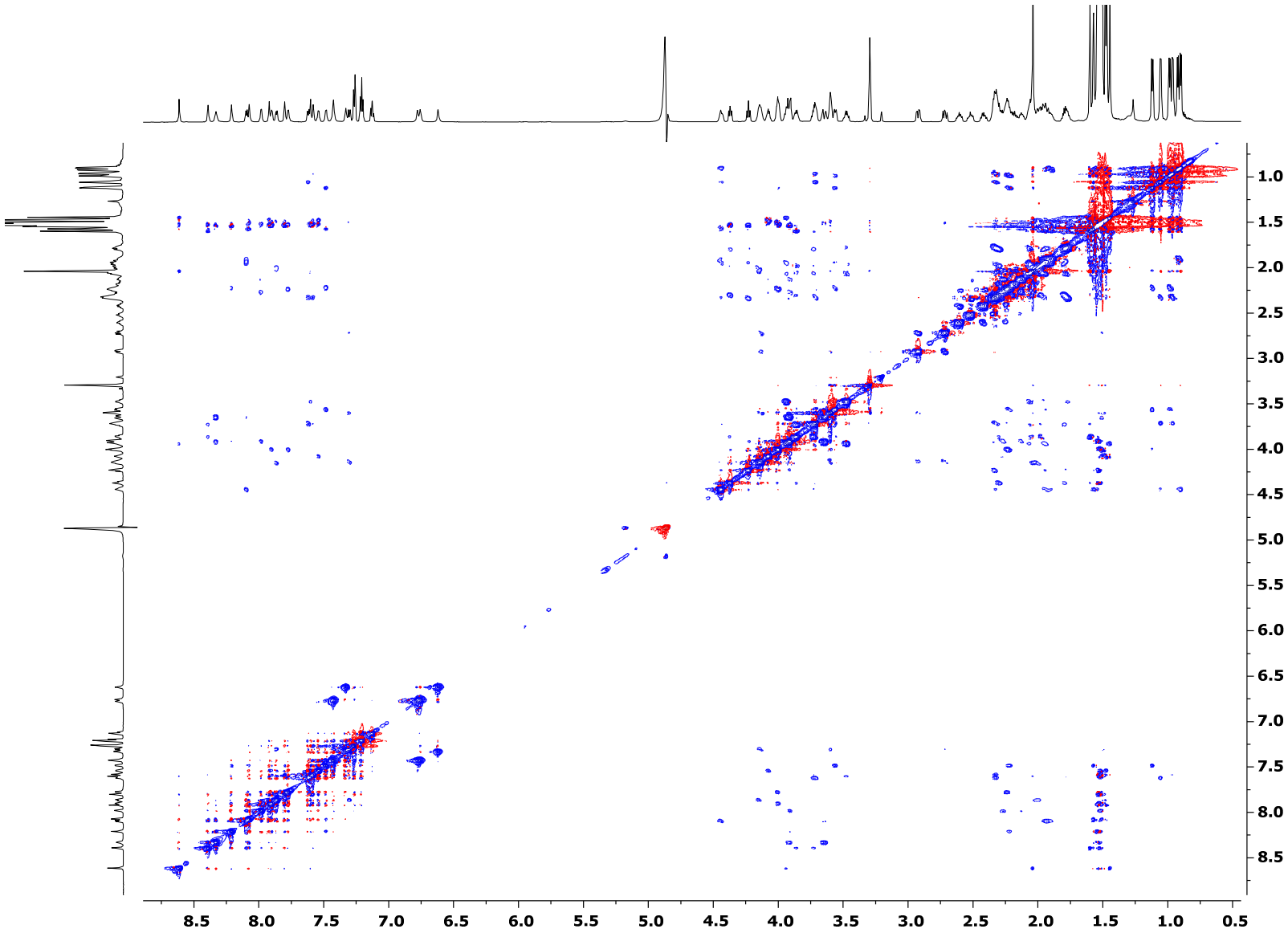

Figure S18. ^{1}H-^{1}H NOESY of alamethicin F50 (**1**) in CD_3OH.

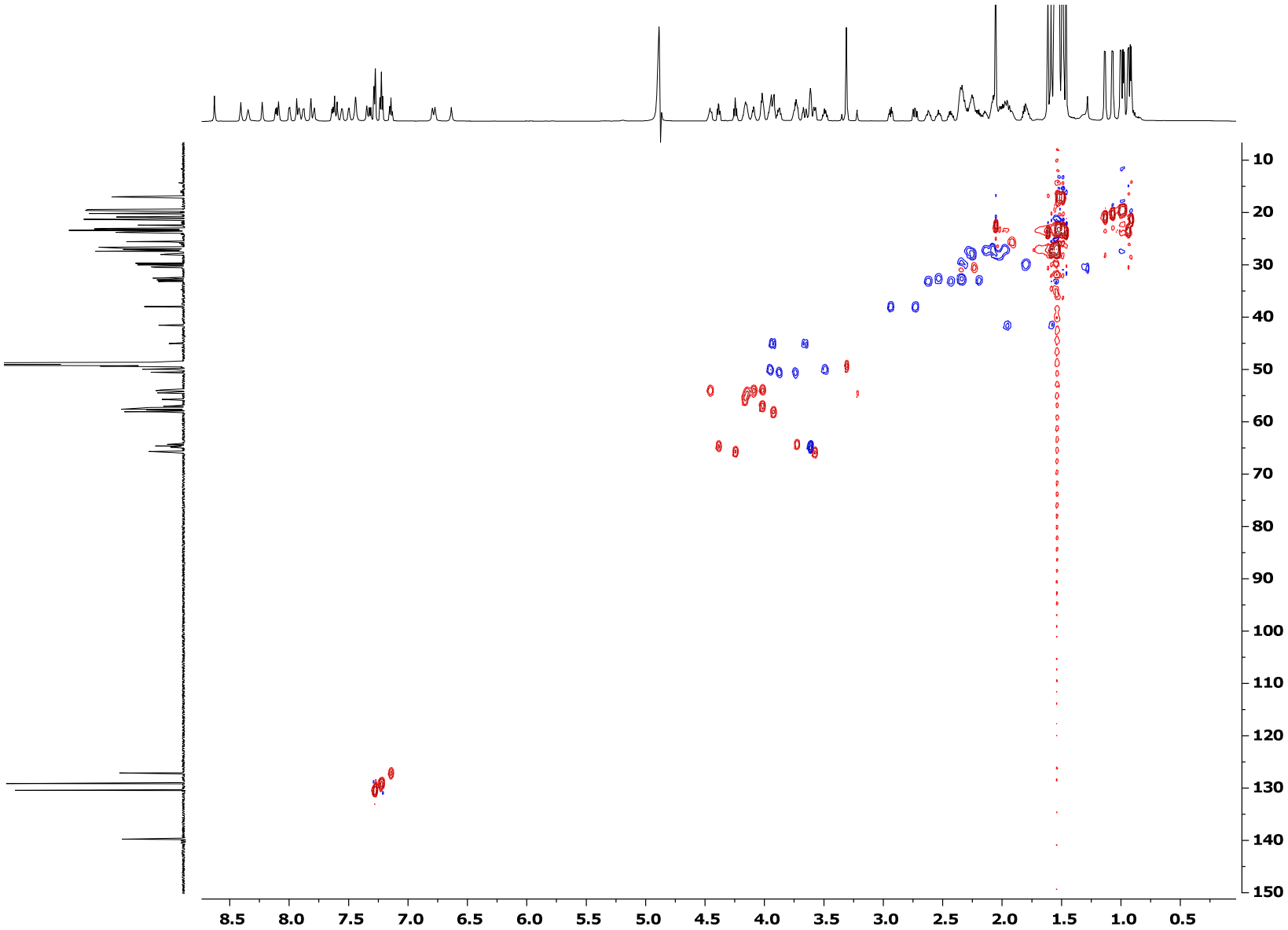

Figure S19. ^{1}H-^{13}C HSQC of alamethicin F50 (**1**) in CD_3OH.

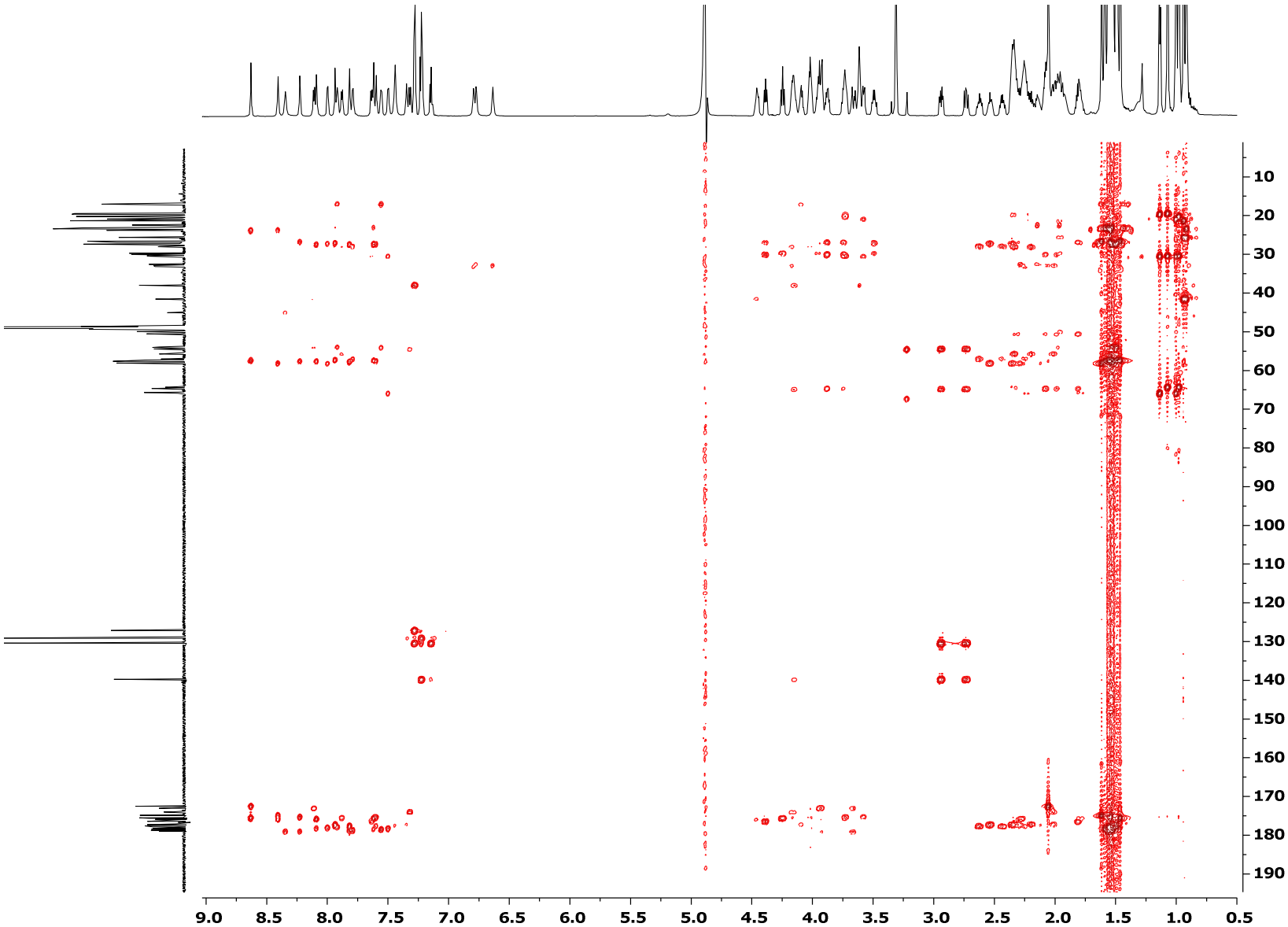

Figure S20. ^{1}H-^{13}C HMBC of alamethicin F50 (**1**) in CD_3OH.

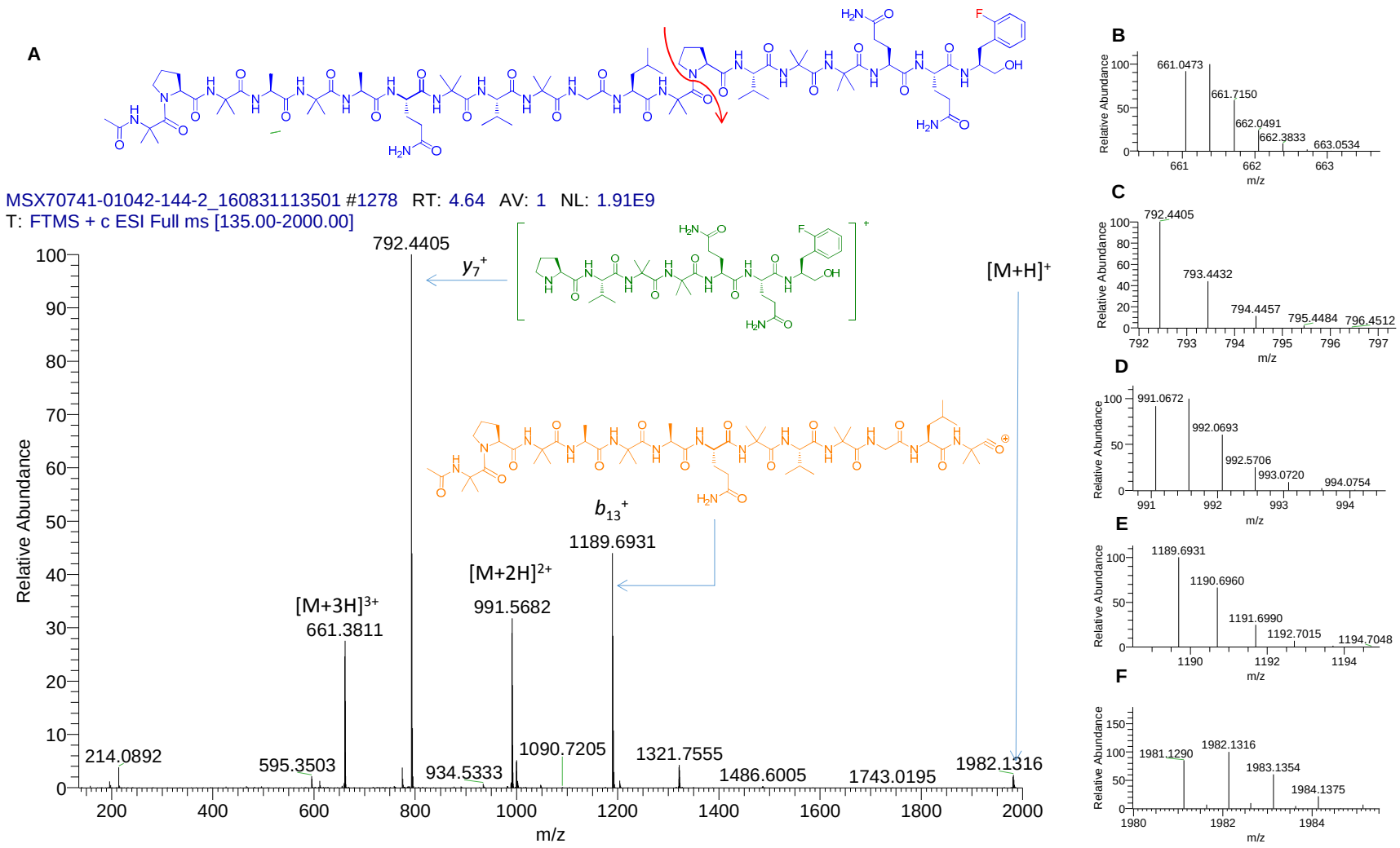

Figure S21. A) Full scan positive HRESIMS of *ortho*-F-Pheol alamethicin F50 (**2**). B-F) Expansion of the $[M+3H]^{3+}$, y_7^+, $[M+2H]^{2+}$, b_{13}^+, and $[M+H]^+$ ion peaks, respectively.

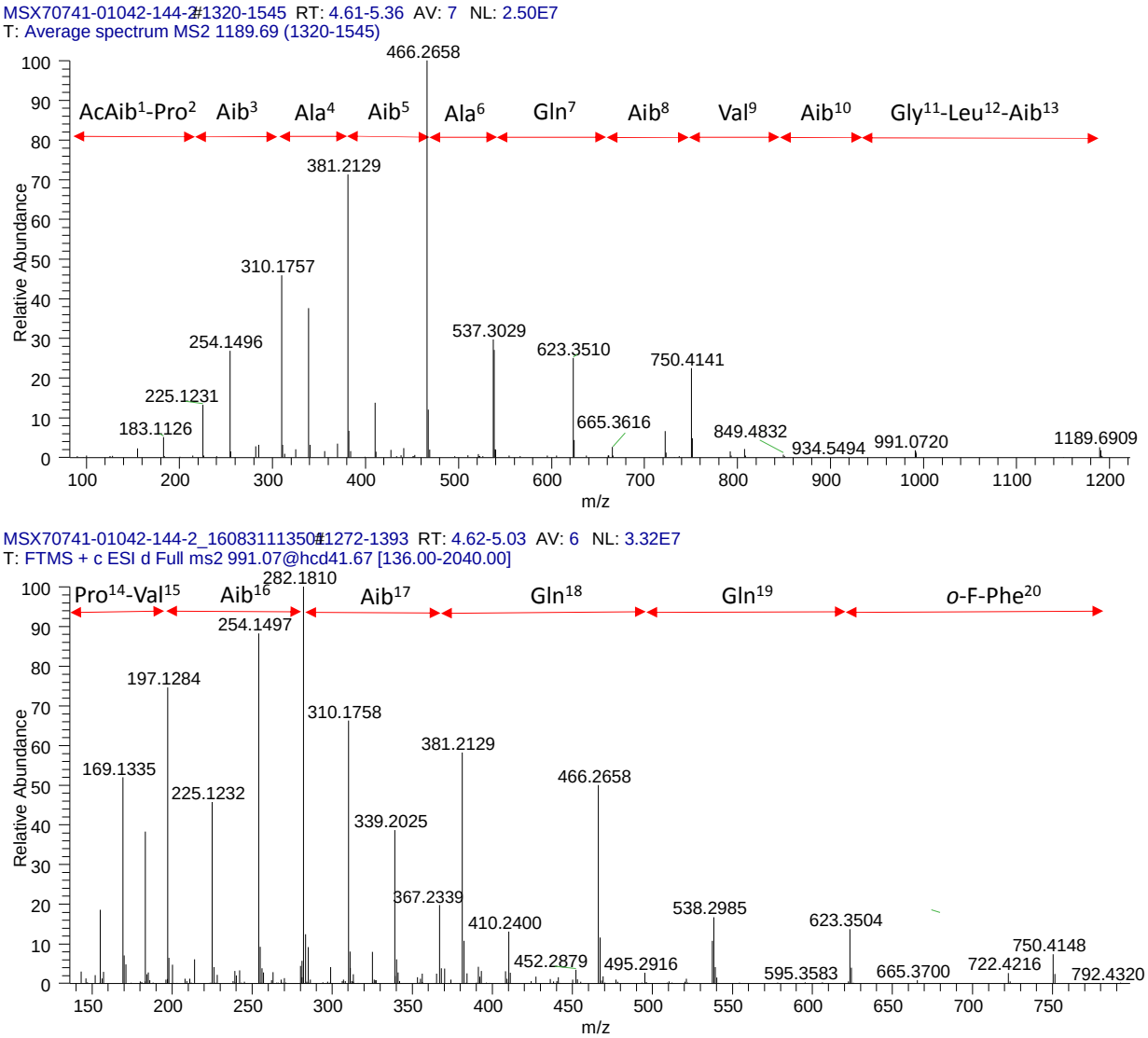

Figure S22. The sequential losses of amino acids for each in-source fragment at *m/z* 1189.69 (top) and *m/z* 792.43 generated from the $[M+2H]^{2+}$ ion (bottom) for compound **2**.

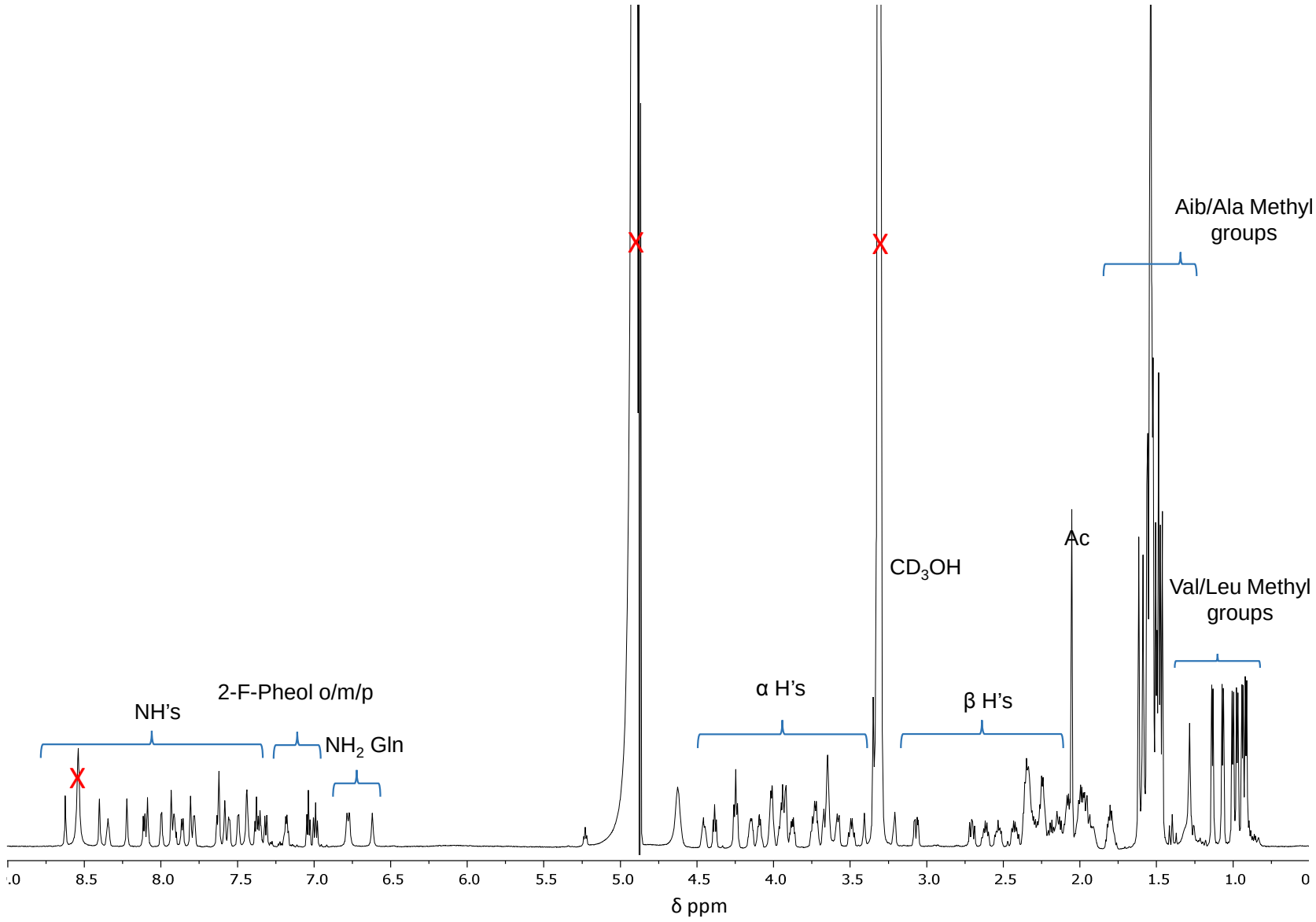

Figure S23. ^{1}H-NMR spectrum of *ortho*-F-Pheol alamethicin F50 (**2**) in CD_3OH (recorded at 700 MHz).

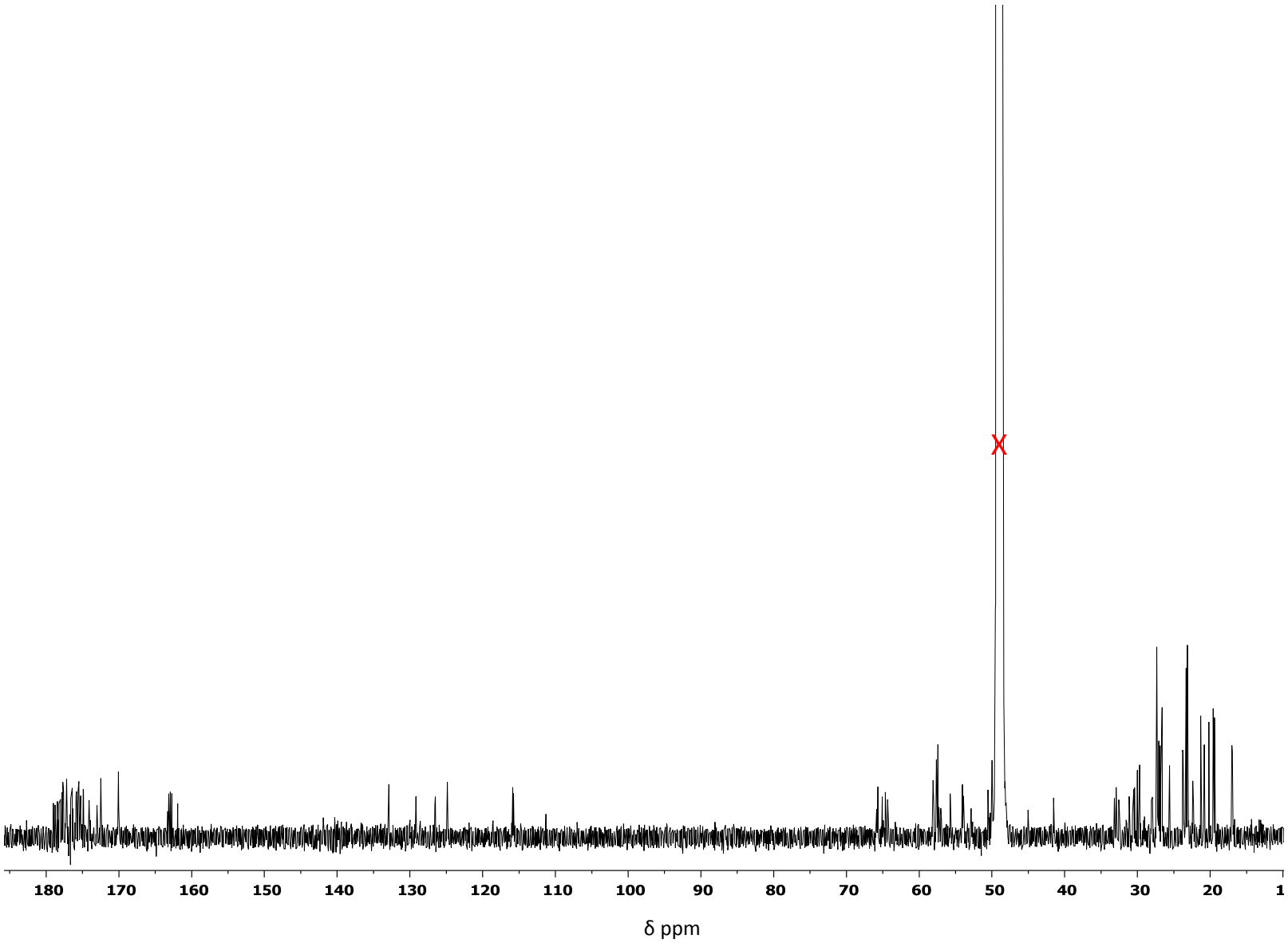

Figure S24. ^{13}C-NMR spectrum of *ortho*-F-Pheol alamethicin F50 (**2**) in CD_3OH (recorded at 175 MHz).

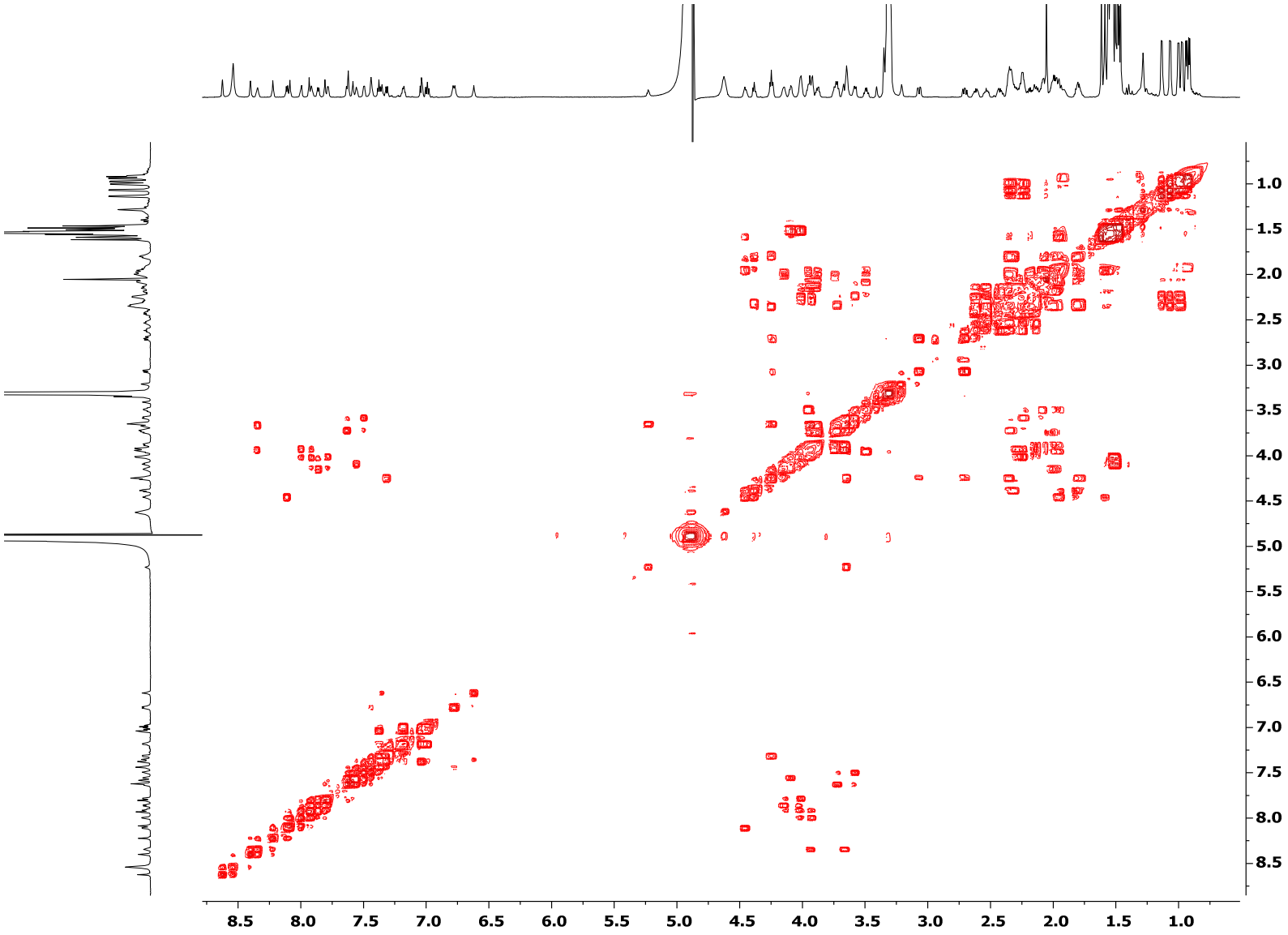

Figure S25. ^{1}H-^{1}H COSY of *ortho*-F-Pheol alamethicin F50 (**2**) in CD_3OH.

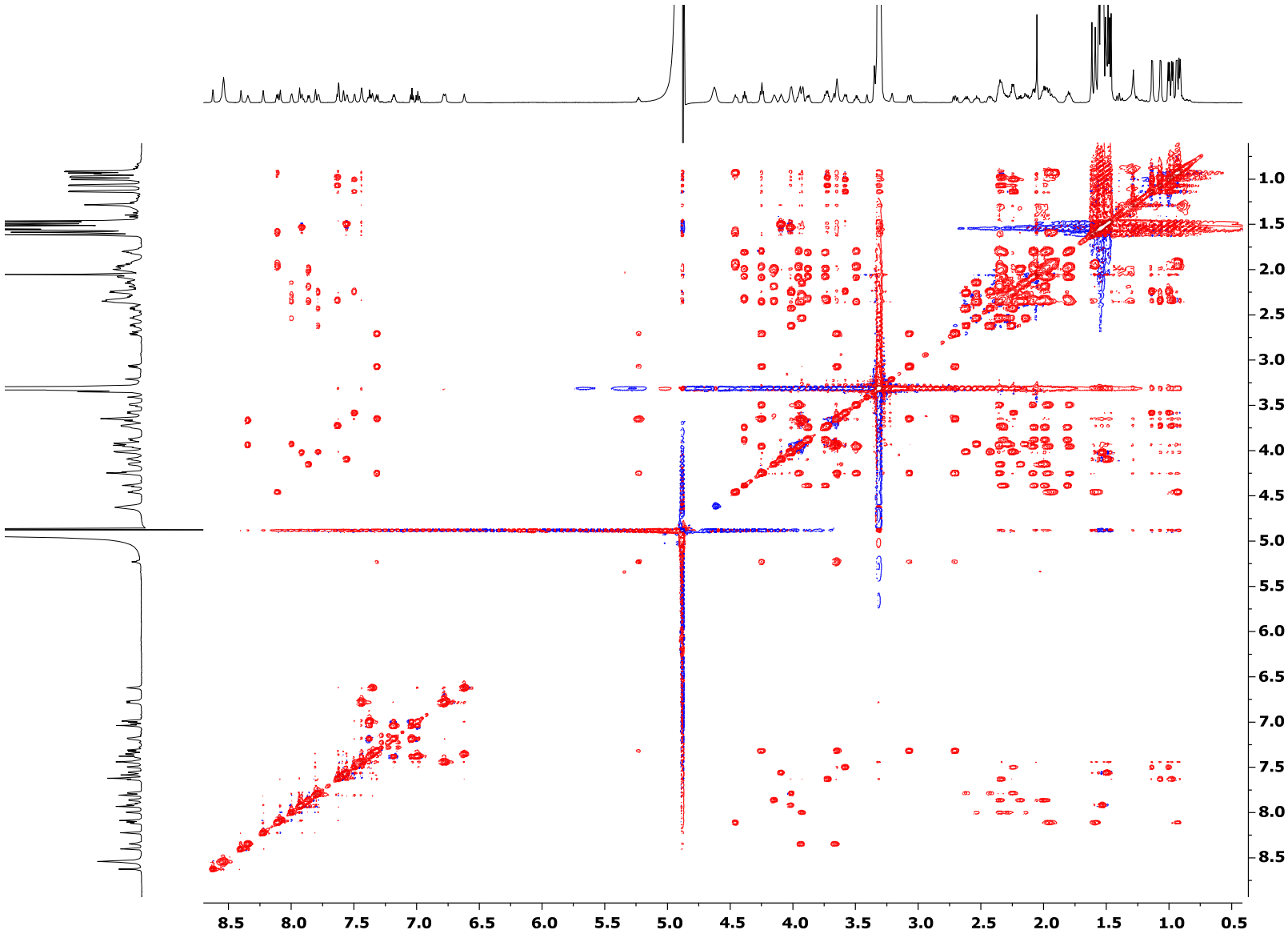

Figure S26. ^{1}H-^{1}H TOCSY of *ortho*-F-Pheol alamethicin F50 (**2**) in CD_3OH.

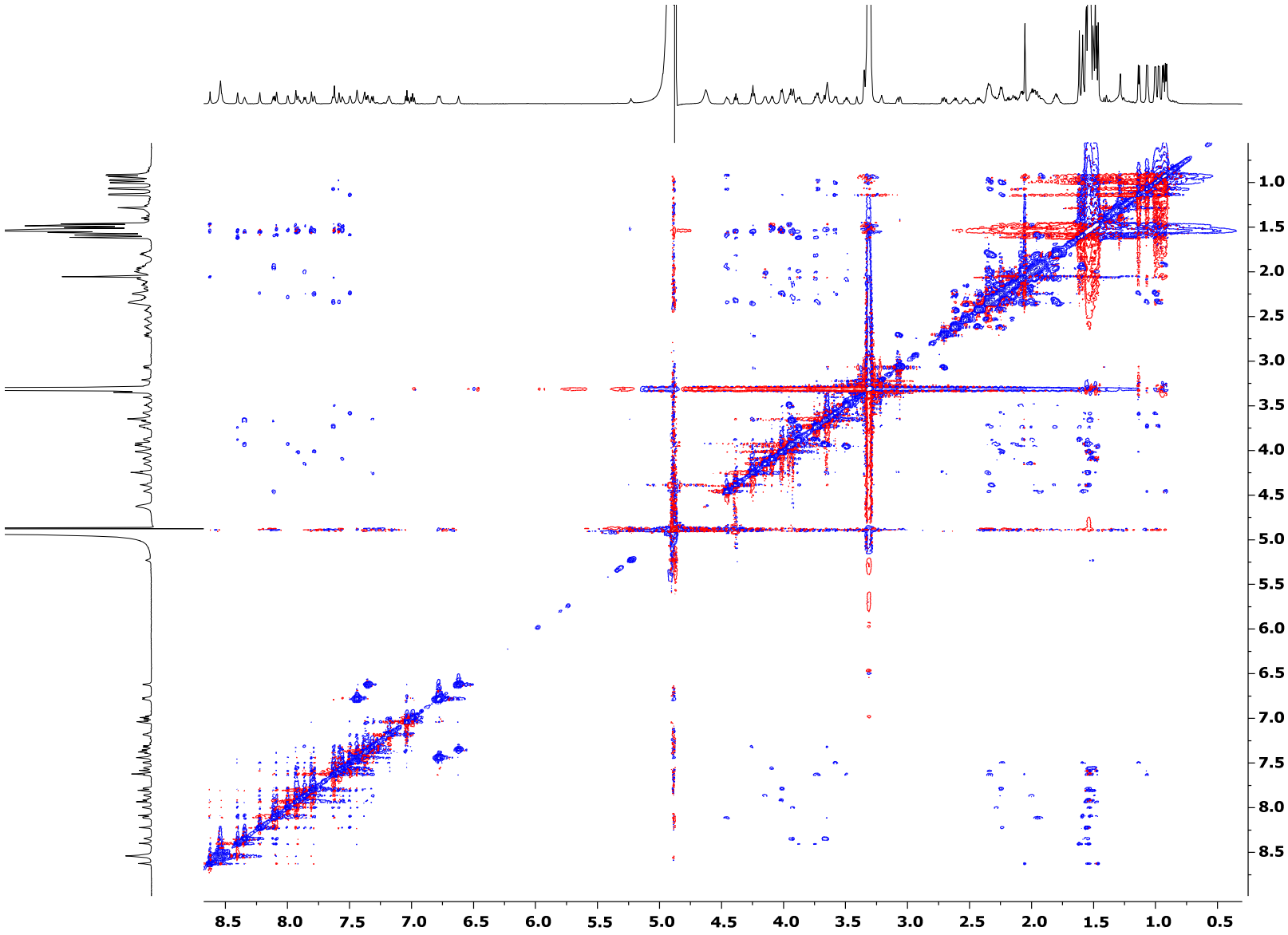

Figure S27. ^{1}H-^{1}H NOESY of *ortho*-F-Pheol alamethicin F50 (**2**) in CD_3OH.

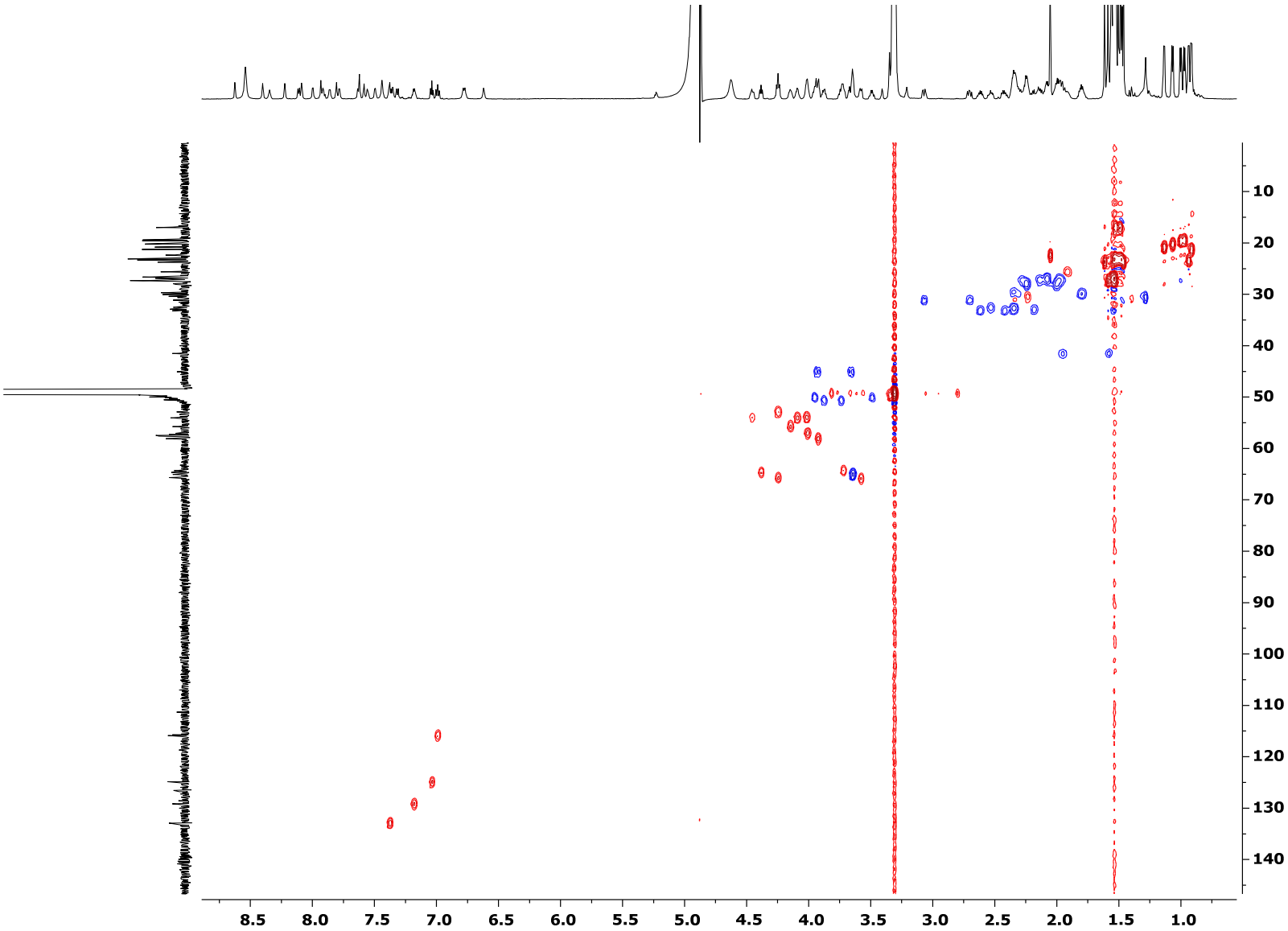

Figure S28. ^{1}H-^{13}C HSQC of *ortho*-F-Pheol alamethicin F50 (**2**) in CD_3OH.

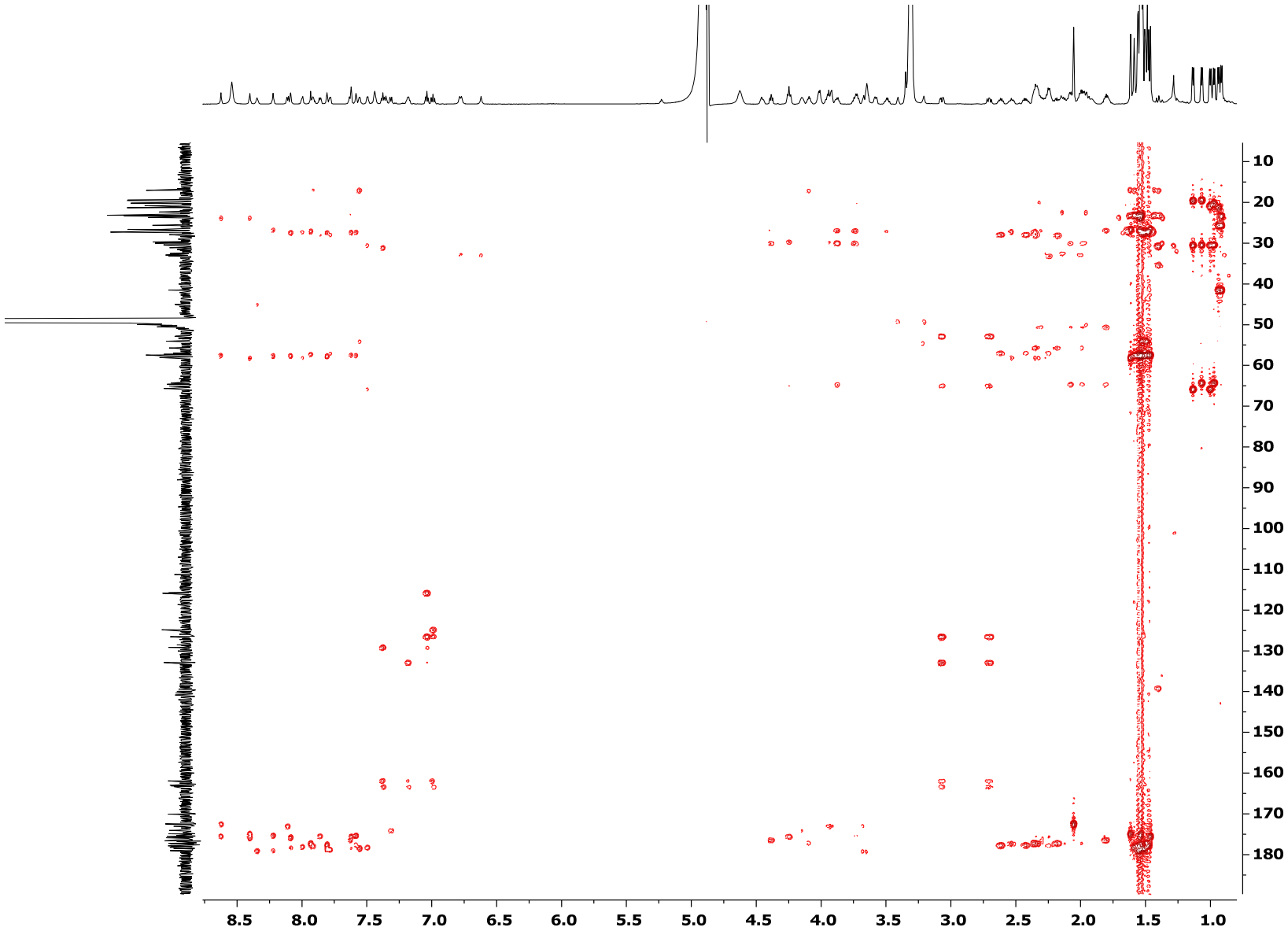

Figure S29. ^{1}H-^{13}C HMBC of *ortho*-F-Pheol alamethicin F50 (**2**) in CD_3OH.

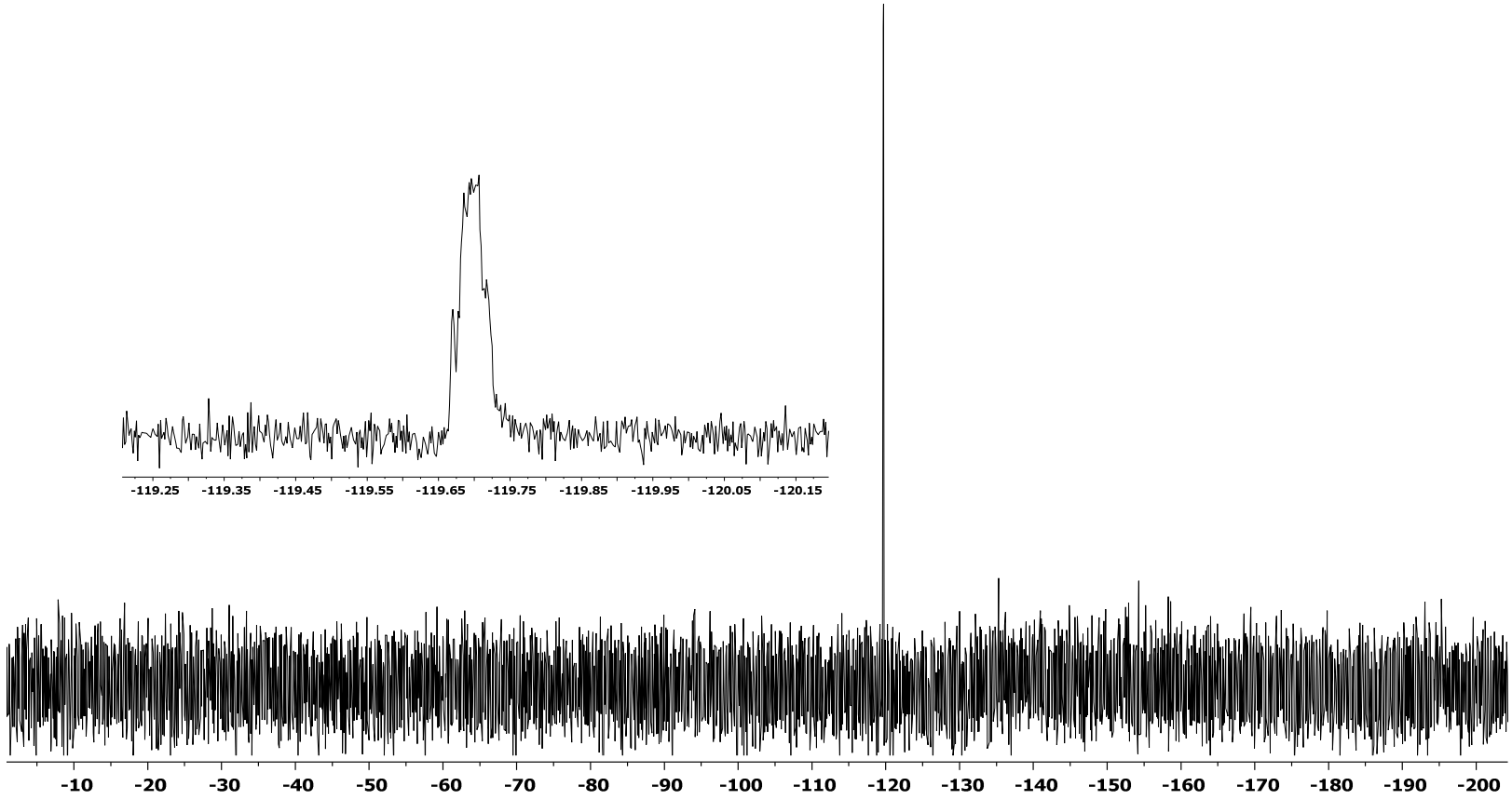

Figure S30. ^{19}F-NMR spectrum of *ortho*-F-Pheol alamethicin F50 (**2**) in CD_3OH (recorded at 470 MHz).

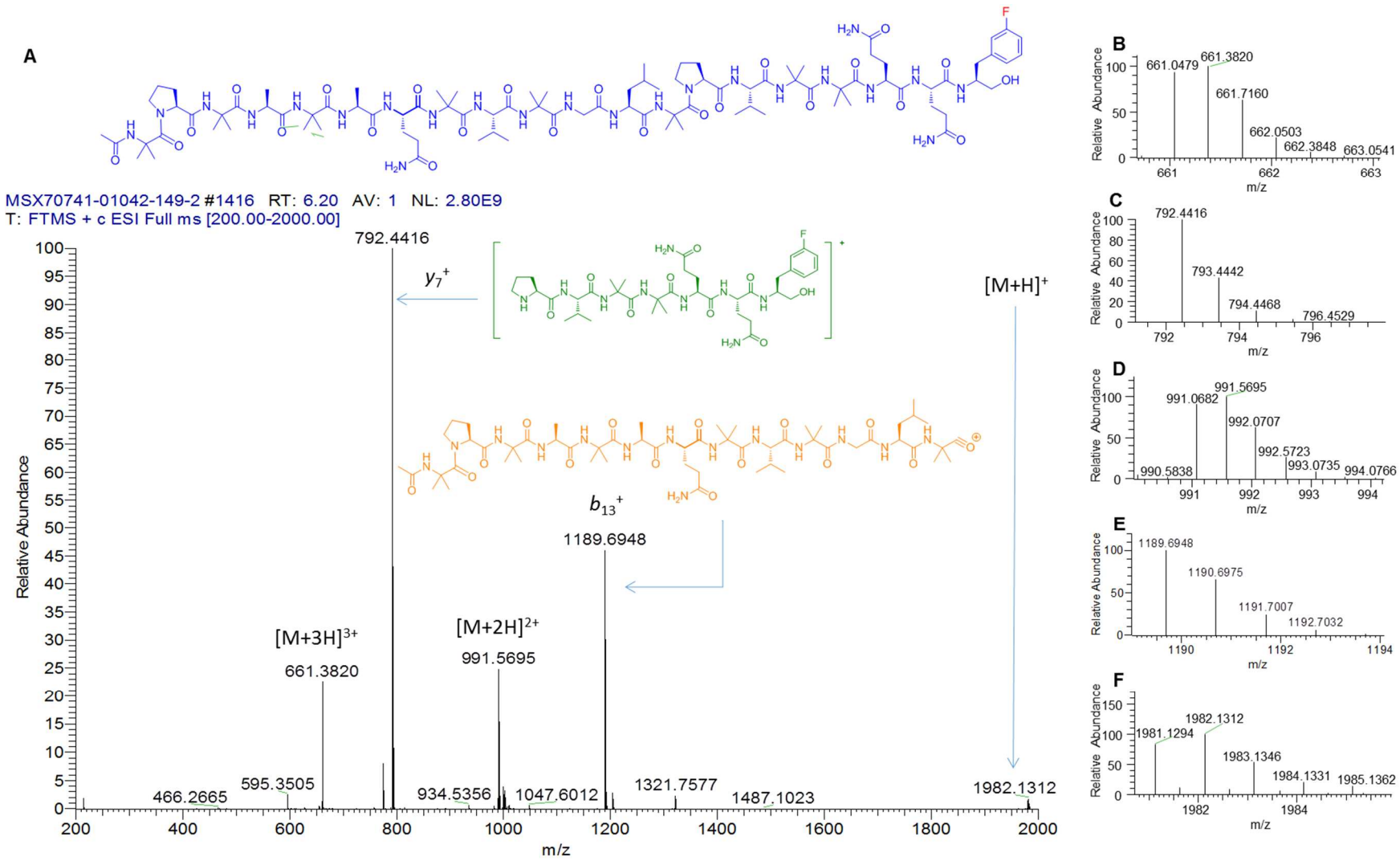

Figure S31. A) Full scan positive HRESIMS of *meta*-F-Pheol alamethicin F50 (**3**). B-F) Expansion of the $[M+3H]^{3+}$, y_7^+, $[M+2H]^{2+}$, b_{13}^+, and $[M+H]^+$ ion peaks, respectively.

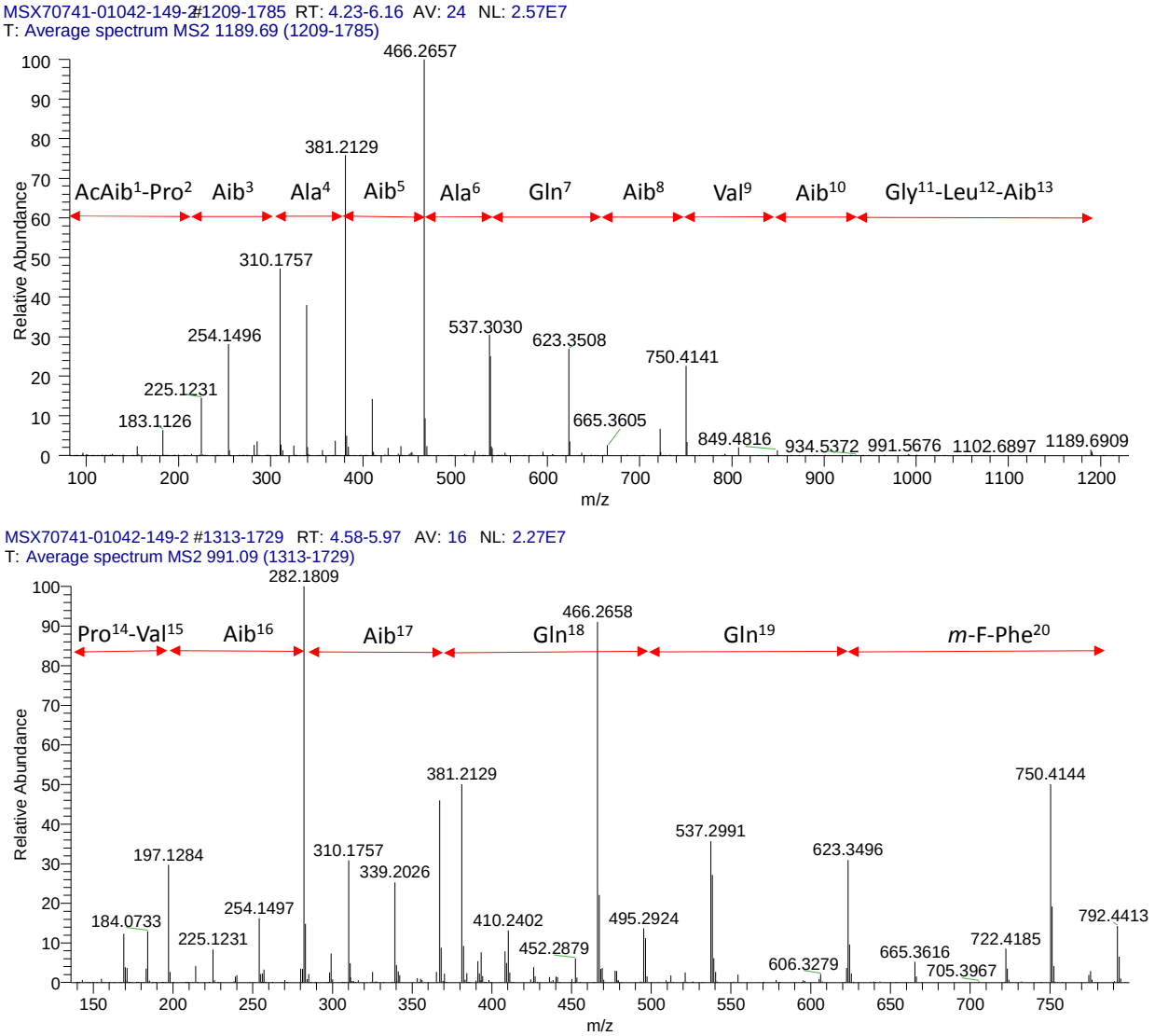

Figure S32. The sequential losses of amino acids for each in-source fragment at *m/z* 1189.69 (top) and *m/z* 792.44 generated from the $[M+2H]^{2+}$ ion (bottom) for compound **3**.

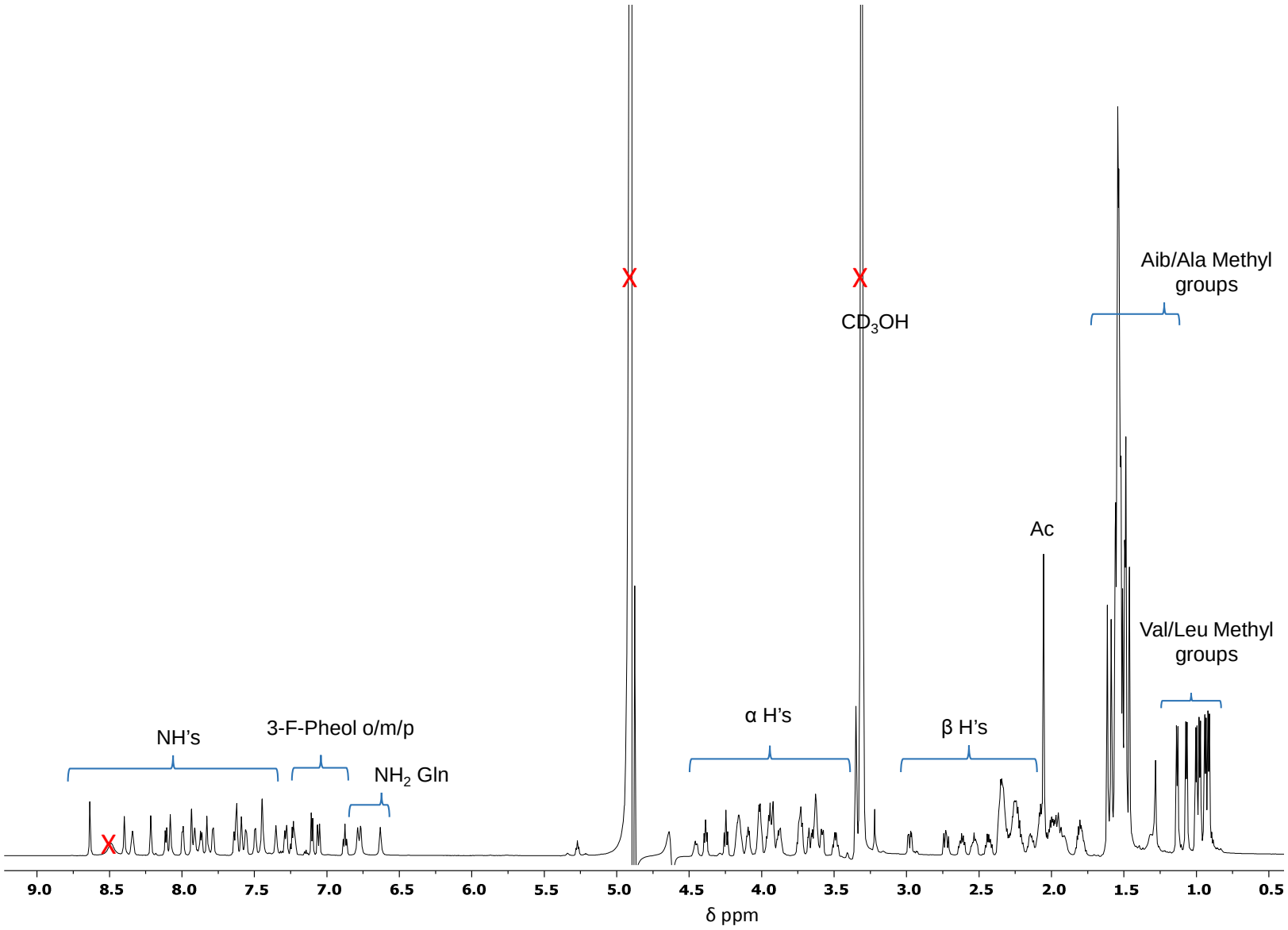

Figure S33. ^{1}H-NMR spectrum of *meta*-F-Pheol alamethicin F50 (**3**) in CD_3OH (recorded at 700 MHz).

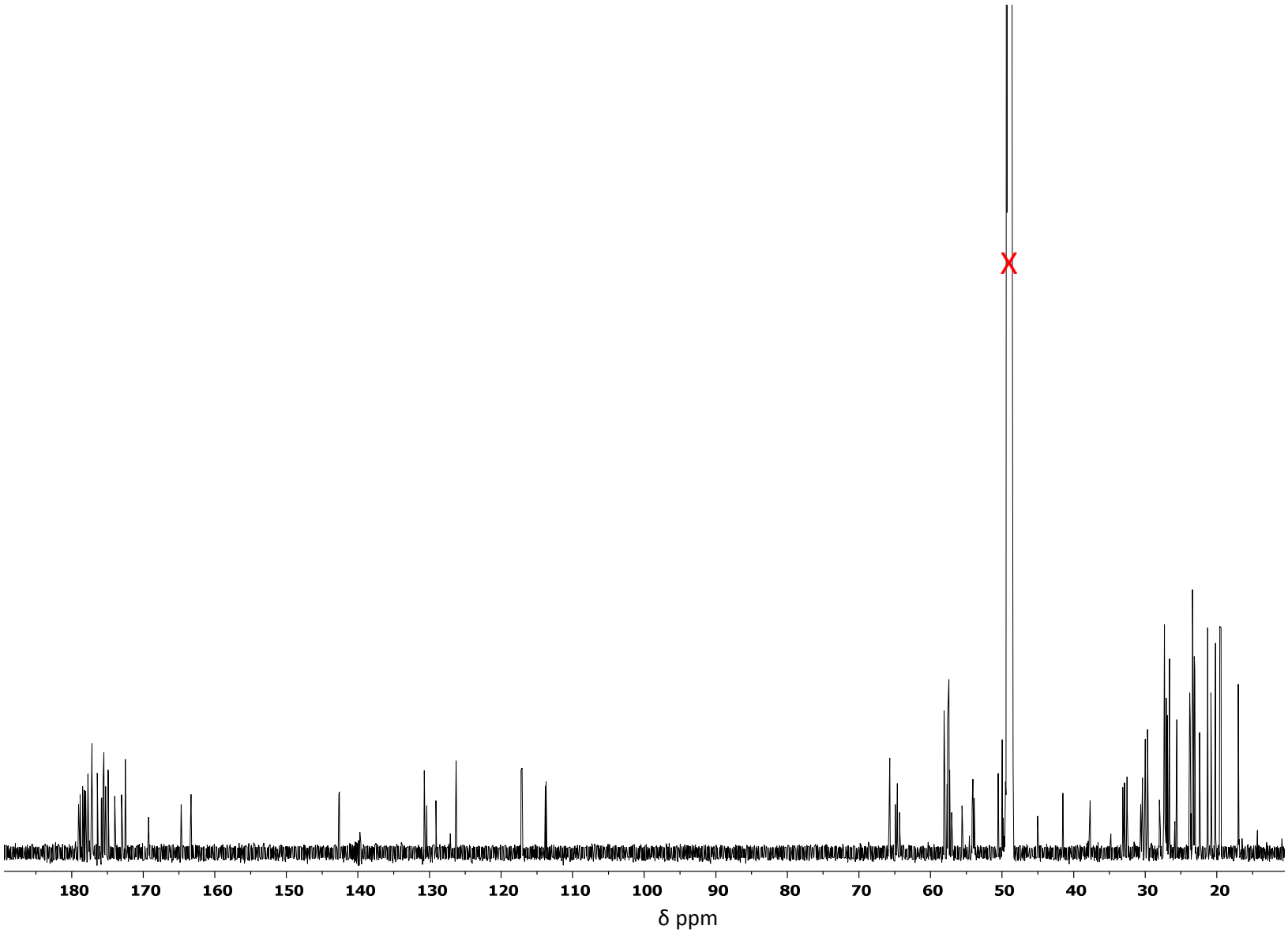

Figure S34. ^{13}C-NMR spectrum of *meta*-F-Pheol alamethicin F50 (**3**) in CD_3OH (recorded at 175 MHz).

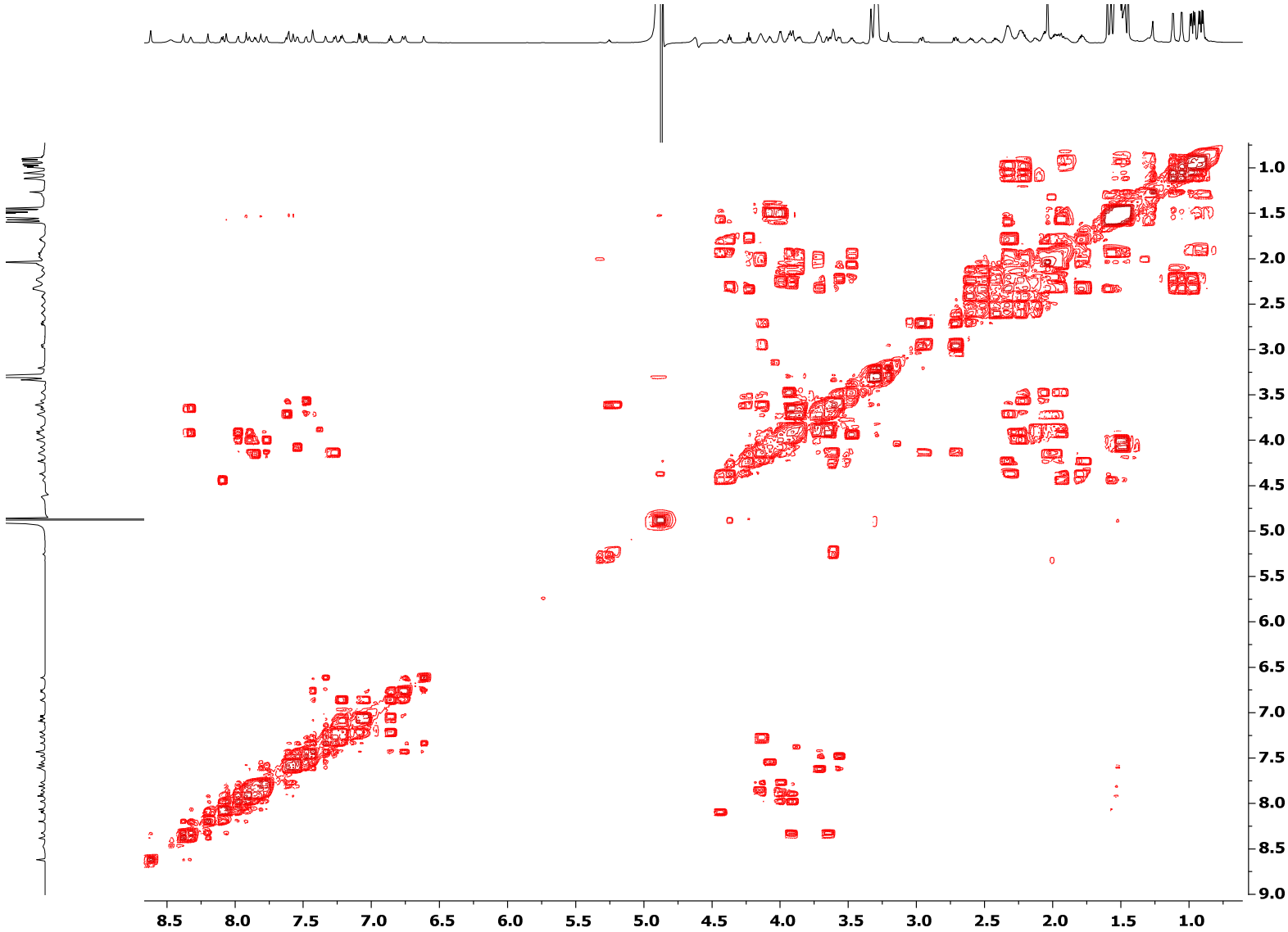

Figure S35. ^{1}H-^{1}H COSY of *meta*-F-Pheol alamethicin F50 (**3**) in CD_3OH.

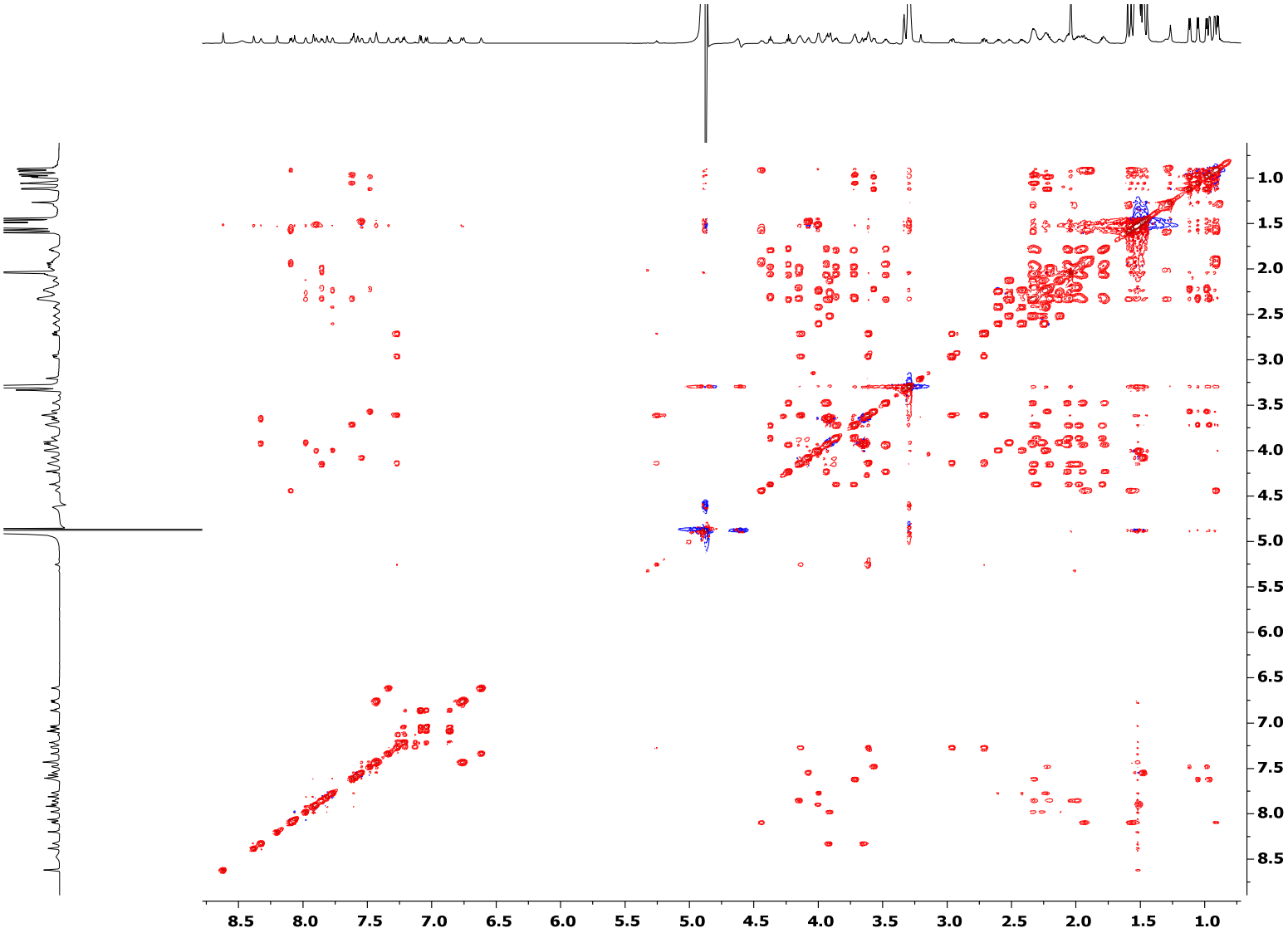

Figure S36. ^{1}H-^{1}H TOCSY of *meta*-F-Pheol alamethicin F50 (**3**) in CD_3OH.

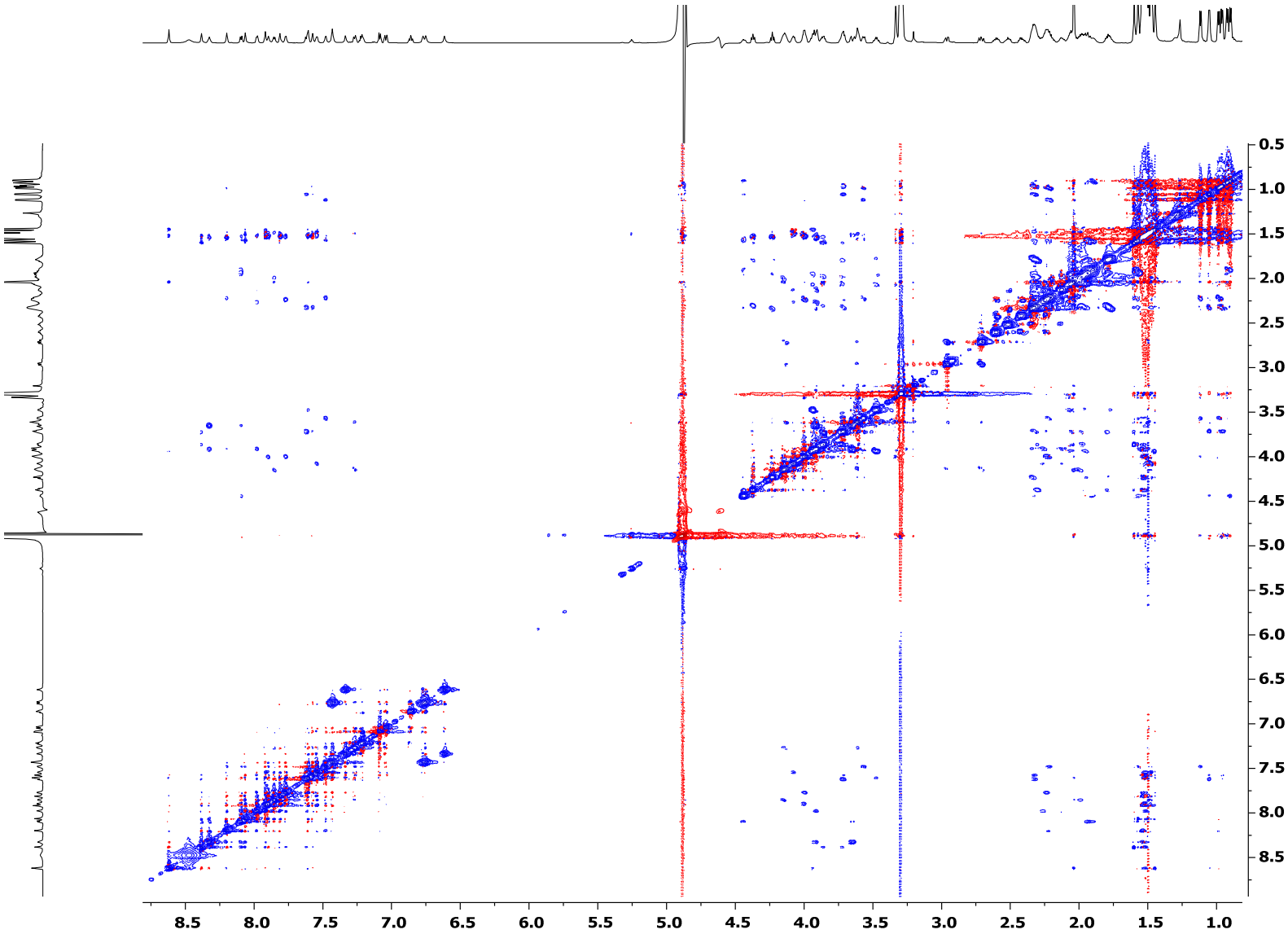

Figure S37. ^{1}H-^{1}H NOESY of *meta*-F-Pheol alamethicin F50 (**3**) in CD_3OH.

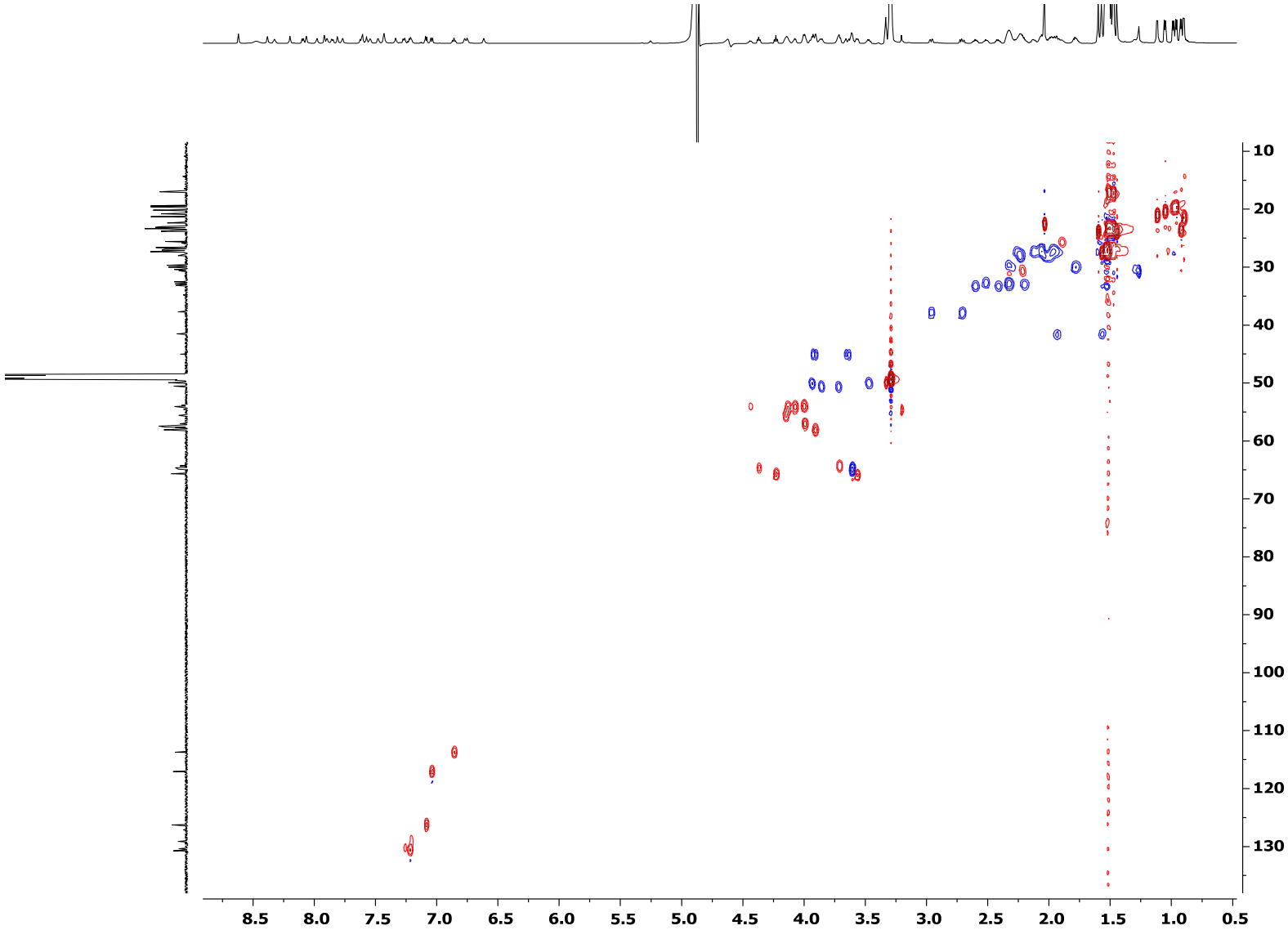

Figure S38. ^{1}H-^{13}C HSQC of *meta*-F-Pheol alamethicin F50 (**3**) in CD_3OH.

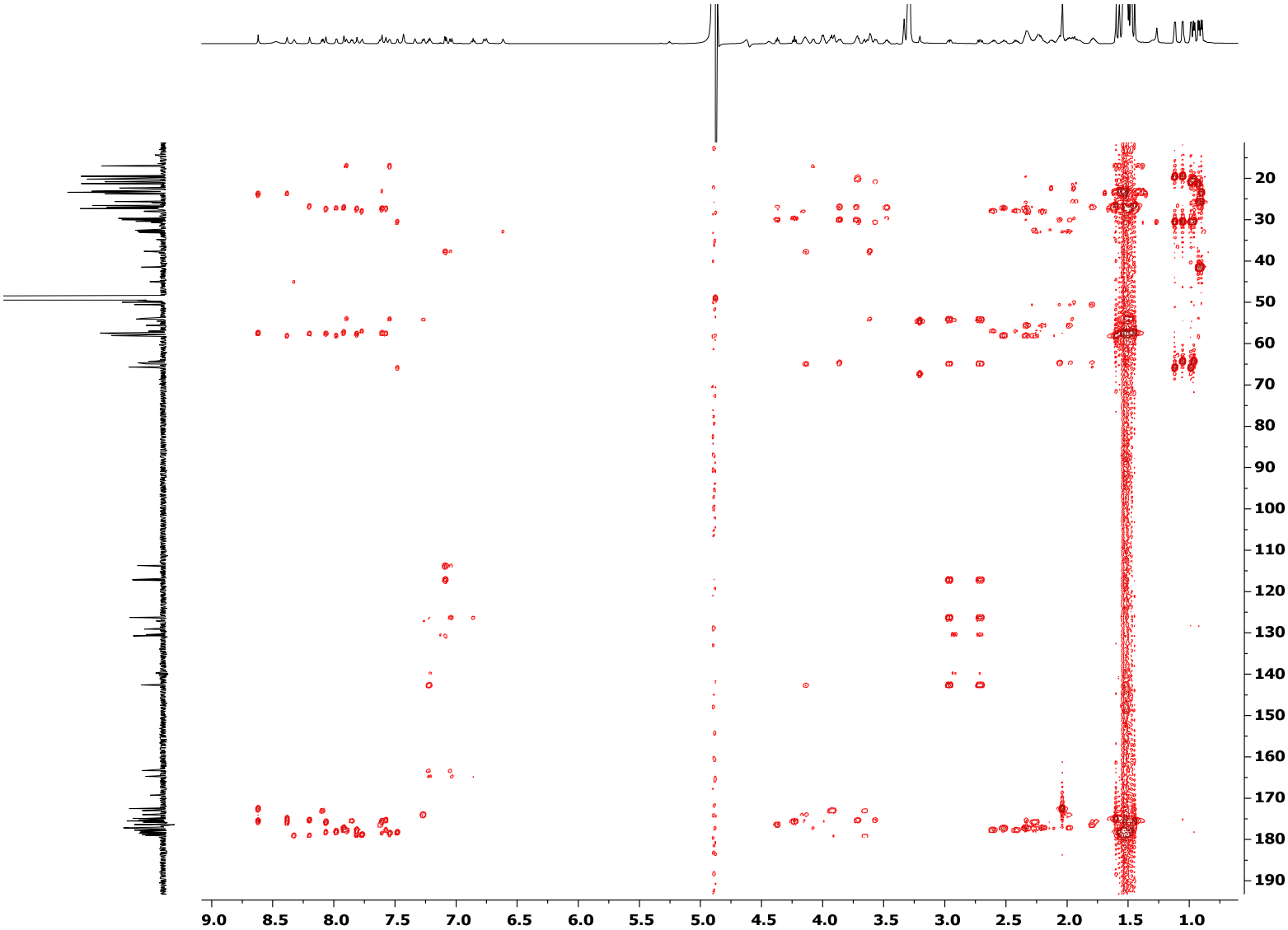

Figure S39. ^{1}H-^{13}C HMBC of *meta*-F-Pheol alamethicin F50 (**3**) in CD_3OH.

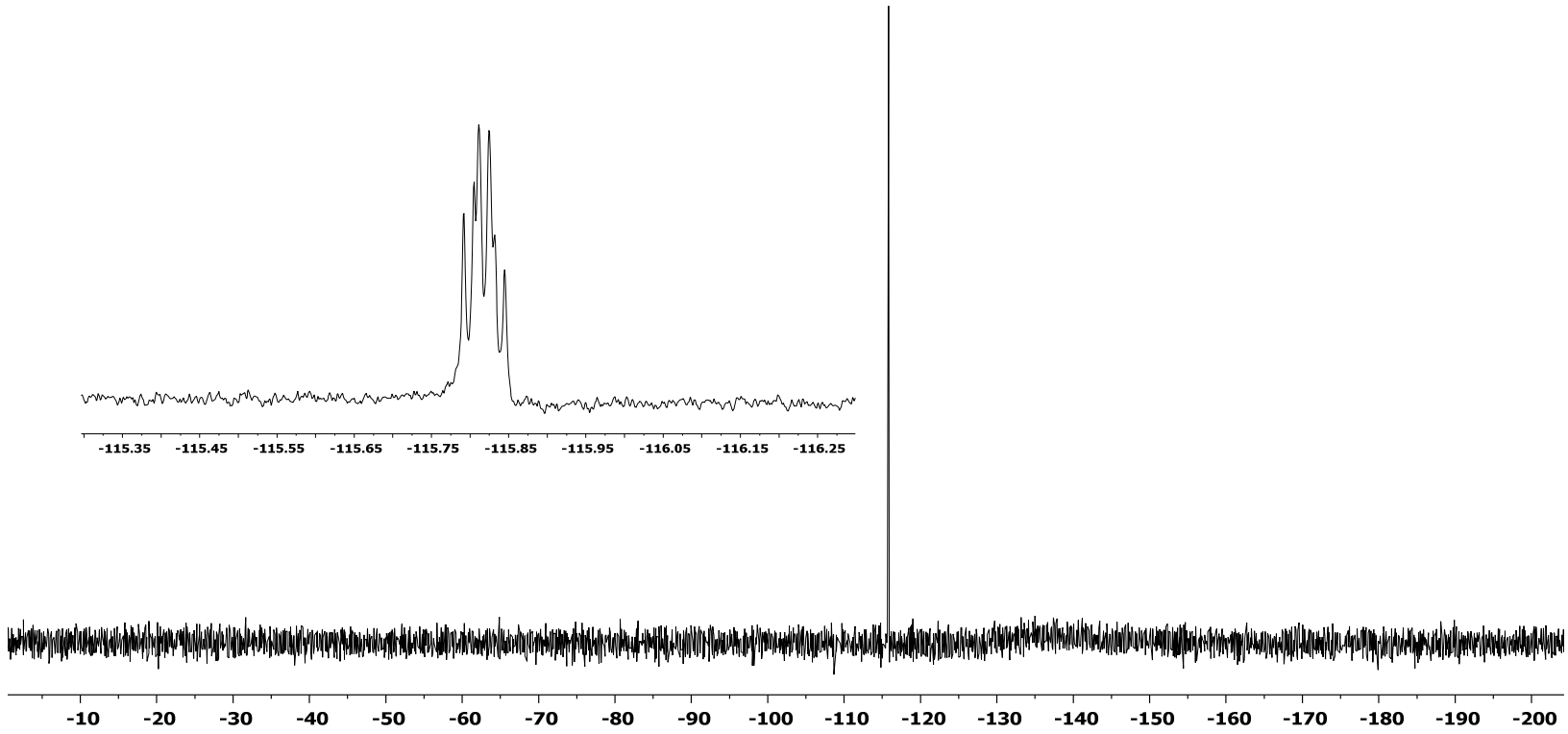

Figure S40. ^{19}F NMR spectrum of *meta*-F-Pheol alamethicin F50 (**3**) in CD_3OH (recorded at 470 MHz).

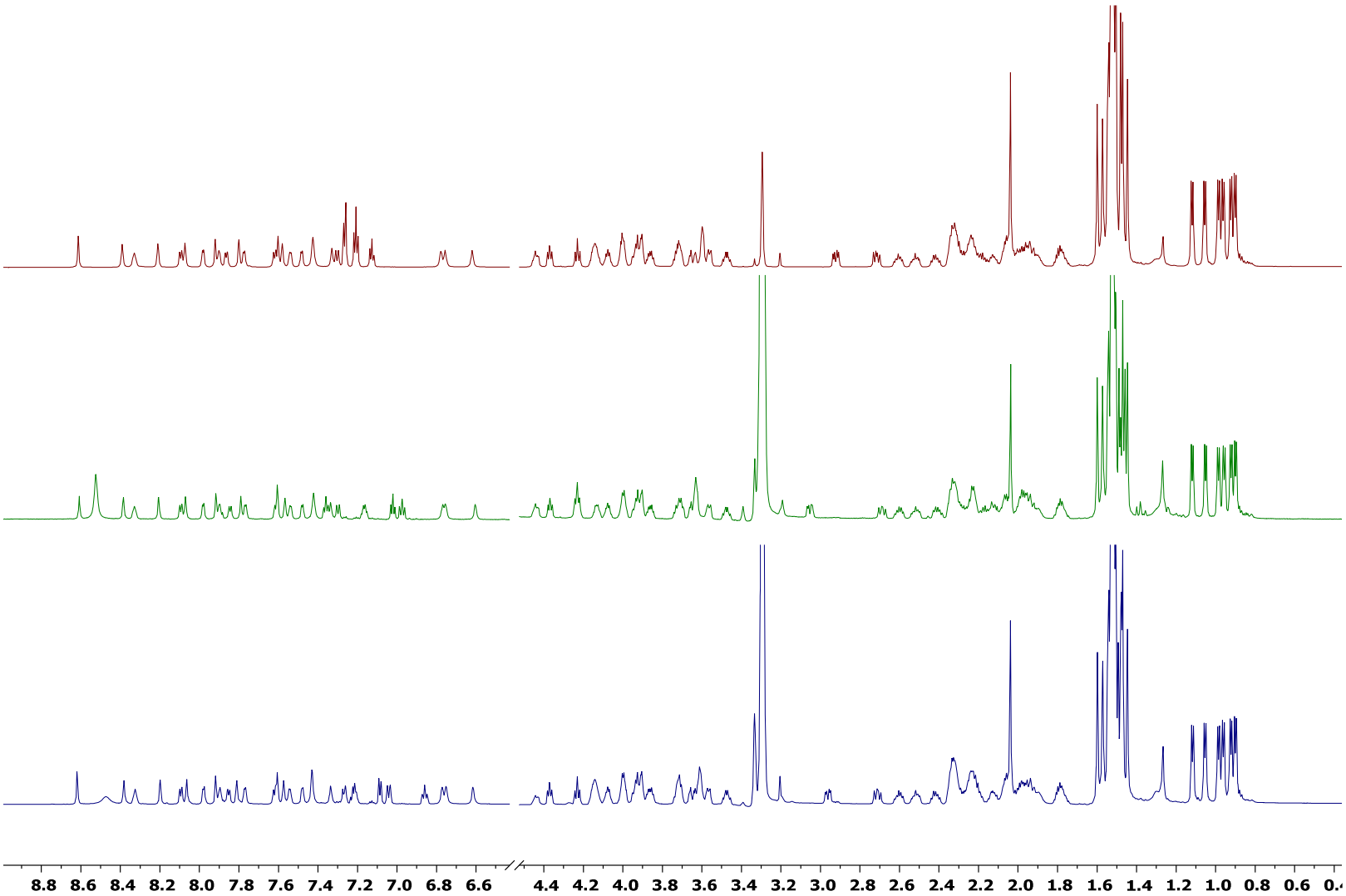

Figure S41. Comparison of the ^{1}H-NMR spectra for compounds **1** (maroon), **2** (green), and **3** (blue). Recorded at 700 MHz in CD_3OH.

References

(1) Ayers, S.; Ehrmann, B. M.; Adcock, A. F.; Kroll, D. J.; Carcache de Blanco, E. J.; Shen, Q.; Swanson, S. M.; Falkinham, J. O., 3rd; Wani, M. C.; Mitchell, S. M.; Pearce, C. J.; Oberlies, N. H. *J. Pept. Sci.* **2012**, *18*, 500-510.

(2) Degenkolb, T.; Dieckmann, R.; Nielsen, K. F.; Gräfenhan, T.; Theis, C.; Zafari, D.; Chaverri, P.; Ismaiel, A.; Brückner, H.; von Döhren, H.; Thrane, U.; Petrini, O.; Samuels, G. J. *Mycol. Prog.* **2008**, *7*, 177-219.

(3) Jaklitsch, W. M.; Voglmayr, H. *Stud. Mycol.* **2015**, *80*, 1-87.

(4) Schoch, C. L.; Robbertse, B.; Robert, V.; Vu, D.; Cardinali, G.; Irinyi, L.; Meyer, W.; Nilsson, R. H.; Hughes, K.; Miller, A. N.; Kirk, P. M.; Abarenkov, K.; Aime, M. C.; Ariyawansa, H. A.; Bidartondo, M.; Boekhout, T.; Buyck, B.; Cai, Q.; Chen, J.; Crespo, A.; Crous, P. W.; Damm, U.; De Beer, Z. W.; Dentinger, B. T.; Divakar, P. K.; Duenas, M.; Feau, N.; Fliegerova, K.; Garcia, M. A.; Ge, Z. W.; Griffith, G. W.; Groenewald, J. Z.; Groenewald, M.; Grube, M.; Gryzenhout, M.; Gueidan, C.; Guo, L.; Hambleton, S.; Hamelin, R.; Hansen, K.; Hofstetter, V.; Hong, S. B.; Houbraken, J.; Hyde, K. D.; Inderbitzin, P.; Johnston, P. R.; Karunarathna, S. C.; Koljalg, U.; Kovacs, G. M.; Kraichak, E.; Krizsan, K.; Kurtzman, C. P.; Larsson, K. H.; Leavitt, S.; Letcher, P. M.; Liimatainen, K.; Liu, J. K.; Lodge, D. J.; Luangsa-ard, J. J.; Lumbsch, H. T.; Maharachchikumbura, S. S.; Manamgoda, D.; Martin, M. P.; Minnis, A. M.; Moncalvo, J. M.; Mule, G.; Nakasone, K. K.; Niskanen, T.; Olariaga, I.; Papp, T.; Petkovits, T.; Pino-Bodas, R.; Powell, M. J.; Raja, H. A.; Redecker, D.; Sarmiento-Ramirez, J. M.; Seifert, K. A.; Shrestha, B.; Stenroos, S.; Stielow, B.; Suh, S. O.; Tanaka, K.; Tedersoo, L.; Telleria, M. T.; Udayanga, D.; Untereiner, W. A.; Dieguez Uribeondo, J.; Subbarao, K. V.; Vagvolgyi, C.; Visagie, C.; Voigt, K.; Walker, D. M.; Weir, B. S.; Weiss, M.; Wijayawardene, N. N.; Wingfield, M. J.; Xu, J. P.; Yang, Z. L.; Zhang, N.; Zhuang, W. Y. *Database (Oxford)* **2014**, *2014*.

(5) White, T., l T. Lee S., and Tylor J.; Academic Press, I., Ed. San Diego California **1990**, p 315-322.

(6) Carbone, I.; Kohn, L. M. *Mycologia.* **1999**, *91*, 553-556.

(7) Jaklitsch, W. M.; Komon, M.; Kubicek, C. P.; Druzhinina, I. S. *Mycologia.* **2006**, *98*, 499-513.

(8) Liu, Y. J.; Hall, B. D. *Proc. Natl. Acad. Sci. U. S. A.* **2004**, *101*, 4507-4512.

(9) Schoch, C. L.; Seifert, K. A.; Huhndorf, S.; Robert, V.; Spouge, J. L.; Levesque, C. A.; Chen, W.; Consortium, F. B. *Proc. Natl. Acad. Sci. U. S. A.* **2012**, *109*, 6241-6246.

(10) Druzhinina, I. S.; Kopchinskiy, A. G.; Komon, M.; Bissett, J.; Szakacs, G.; Kubicek, C. P. *Fungal. Genet. Biol.* **2005**, *42*, 813-828.

(11) Bissett, J.; Gams, W.; Jaklitsch, W.; Samuels, G. J. *IMA Fungus* **2015**, *6*, 263-295.

(12) Elike Lieckfeldt, K. A. S. *Stud. Mycol.* **2000**, *45*, 35-44.

(13) Rehner, S. A.; Buckley, E. *Mycologia.* **2005**, *97*, 84-98.

(14) Edgar, R. C. *Nucleic Acids Res.* **2004**, *32*, 1792-1797.

(15) Liu, Y. J.; Whelen, S.; Hall, B. D. *Mol. Biol. Evol.* **1999**, *16*, 1799-1808.

(16) Stamatakis, A. *Bioinformatics.* **2006**, *22*, 2688-2690.

(17) Miller, M. A.; Pfeiffer, W.; Schwartz, T. In *Proceedings of the 2011 TeraGrid Conference: Extreme Digital Discovery*; ACM: Salt Lake City, Utah, 2011, p 1-8.